
Article:
Tong, Meixuezi, Lee, Kyounghee, Ezer, Daphne et al. (9 more authors) (2020) The Evening Complex establishes repressive chromatin domains via H2A.Z deposition. Plant Physiology. pp. 612-625. ISSN 0032-0889

https://doi.org/10.1104/pp.19.00881

Short title: EC-dependent H2A.Z deposition

Corresponding authors: Paloma Mas (paloma.mas@cragenomica.es), Philip A. Wigge (wigge@igzev.de), Pil Joon Seo (pjseo1@snu.ac.kr)

The Evening Complex establishes repressive chromatin domains via H2A.Z deposition

Meixuezi Tong[1,†], Kyounghee Lee[2,†], Daphne Ezer[1], Sandra Cortijo[1], Jaehoon Jung[1,2], Varodom Charoensawan[1], Mathew S. Box[1], Katja E. Jaeger[1], Nozomu Takahashi[3], Paloma Mas[3,4,*], Philip A. Wigge[1,5,*], Pil Joon Seo[2,6,7,*]

[1]Sainsbury Laboratory, University of Cambridge, 47 Bateman St., Cambridge CB2 1LR, UK

[2]Department of Biological Sciences, Sungkyunkwan University, Suwon 16419, Republic of Korea

[3]Center for Research in Agricultural Genomics (CRAG), Consortium CSIC-IRTA-UAB-UB, Parc de Recerca Universitat Autònoma de Barcelona (UAB), Bellaterra (Cerdanyola del Vallés), Barcelona, Spain

[4]Consejo Superior de Investigaciones Científicas (CSIC), Barcelona, Spain

[5]Leibniz-Institut für Gemüse- und Zierpflanzenbau (IGZ), Theodor-Echtermeyer-Weg 1, 14979 Großbeeren, Germany

[6]Department of Chemistry, Seoul National University, Seoul 08826, Republic of Korea

[7]Plant Genomics and Breeding Institute, Seoul National University, Seoul 08826, Republic of Korea

[†]These authors contributed equally to this work.

[*]Corresponding authors: P.M. (paloma.mas@cragenomica.es), P.W. (wigge@igzev.de), or P.J.S. (pjseo1@snu.ac.kr)

The author responsible for distribution of materials integral to the findings presented in this article in accordance with the policy described in the Instructions for Authors (www.plantphysiol.org) is: P.M. (paloma.mas@cragenomica.es), P.W. (wigge@igzev.de), or P.J.S. (pjseo1@snu.ac.kr).

One sentence summary: The Evening Complex interacts with the complex responsible for the deposition of the histone variant H2A.Z, creating repressive chromatin domains to repress a cohort of target genes in *Arabidopsis*.

Author contributions: PW, PM, and PJS participated in the design of the study and wrote the manuscript. MT, KL, and NT performed the molecular experiments. MT and DE performed the analysis of sequencing data. MT, SC, JJ, VC, and MSB performed large-scale time-course experiments. MT and KEJ performed ChIP-seq experiments. PW, PM, and PJS conceived the project. All authors read and approved the final manuscript.

Abstract

The Evening Complex (EC) is a core component of the Arabidopsis (*Arabidopsis thaliana*) circadian clock, which represses target gene expression at the end of the day and integrates temperature information to coordinate environmental and endogenous signals. Here we show that the EC induces repressive chromatin structure to regulate the evening transcriptome. The EC component ELF3 directly interacts with a protein from the SWI2/SNF2-RELATED (SWR1) complex to control deposition of H2A.Z-nucleosomes at the EC target genes. SWR1 components display circadian oscillation in gene expression with a peak at dusk. In turn, SWR1 is required for the circadian clockwork, as defects in SWR1 activity alter morning-expressed genes. The EC-SWR1 complex binds to the loci of the core clock genes *PSEUDO-RESPONSE REGULATOR7* (*PRR7*) and *PRR9* and catalyzes deposition of nucleosomes containing the histone variant H2A.Z coincident with the repression of these genes at dusk. This provides a mechanism by which the circadian clock temporally establishes repressive chromatin domains to shape oscillatory gene expression around dusk.

Keywords Chromatin remodeling, circadian clock, Evening Complex, H2A.Z, SWR1

Introduction

The circadian clock generates biological rhythms with a period of approximately 24 hours to coordinate plant growth and development with environmental cycles (Greenham and McClung, 2015). A large fraction of the Arabidopsis (*Arabidopsis thaliana*) transcriptome is circadian-regulated (Staiger and Green, 2011). Circadian transcription allows the molecular anticipation of the environmental cycles, which improves plant fitness and adaptation (Yerushalmi et al., 2011). Consistent with its adaptive function, the circadian clock is subject to multiple layers of regulation, which contribute towards accurate oscillations (Seo and Mas, 2014).

Transcriptional regulation of circadian genes is a basic framework of clock architecture (Carre and Kim, 2002; Salome and McClung, 2004). The Arabidopsis central oscillator consists of a series of sequential regulatory loops composed of genes expressed at different times during the diurnal cycle. Morning-expressed genes such as *CIRCADIAN CLOCK-ASSOCIATED 1* (*CCA1*) and *LATE ELONGATED HYPOCOTYL* (*LHY*) repress the expression of evening-expressed genes like *TIMING OF CAB EXPRESSION 1/PSEUDO-RESPONSE REGULATOR 1* (*TOC1/PRR1*) (Alabadi et al., 2001), while in turn the TOC1 protein represses *CCA1* and *LHY* during the night (Alabadi et al., 2001; Gendron et al., 2012; Huang et al., 2012; Pokhilko et al., 2013). Repression of *CCA1* and *LHY* throughout the day also occurs by the sequential action of additional members of the PRR family, including PRR9, PRR7, and PRR5 (Nakamichi et al., 2010; Salome et al., 2010). Additional repressors of morning gene expression include the components of the Evening Complex (EC), EARLY FLOWERING 3 (ELF3), ELF4, and LUX ARRYTHMO/PHYTOCLOCK 1 (LUX/PCL1) (Nusinow et al., 2011; Chow et al., 2012; Herrero et al., 2012).

The EC is a core component of the circadian clock, and *elf3* mutants are arrhythmic

87 under continuous light (Hicks et al., 1996; Lu et al., 2012). By binding to the promoters of
88 hundreds of key regulators of circadian clock, photosynthesis, and phytohormone signaling,
89 the EC is able to repress their expression (Ezer et al., 2017). Because the activity of the EC is
90 reduced at warmer temperatures, and environmental sensing phytochromes co-bind target
91 promoters, the EC is able to integrate environmental information into endogenous
92 developmental programs (Ezer et al., 2017). However, the molecular mechanisms by which
93 the EC represses gene expression are not known.

94 Histone variants influence chromatin structure and therefore transcription. H2A.Z is
95 the most well-conserved histone variant, enriched near transcription start sites (TSSs)
96 (Raisner et al., 2005; Raisner and Madhani, 2006) and influencing transcriptional activities of
97 associated genes (Raisner et al., 2005). Effects of H2A.Z deposition are likely variable
98 depending on chromatin context: H2A.Z deposition at promoters prevents the spread of
99 heterochromatin in yeast and is associated with transcriptional inducibility (Guillemette et al.,
100 2005), whereas in metazoans, H2A.Z has been shown to play a role in heterochromatin
101 formation and maintenance (Rangasamy et al., 2003; Swaminathan et al., 2005). In plants,
102 H2A.Z-nucleosomes confer transcriptional competence (Deal et al., 2007; To and Kim, 2014),
103 and also appear to wrap DNA more tightly, facilitating inducible gene expression (Kumar and
104 Wigge, 2010; Coleman-Derr and Zilberman, 2012).

105 The Arabidopsis genome encodes putative homologs of catalytic subunits of the
106 Swi2/Snf2-Related (SWR1) / Swi2/Snf2-Related CBP Activator Protein (SRCAP) complex
107 responsible for H2A.Z deposition, including PHOTOPERIOD-INDEPENDENT EARLY
108 FLOWERING 1 (PIE1), ACTIN-RELATED PROTEIN 6 (ARP6), and SERRATED LEAVES
109 AND EARLY FLOWERING (SEF) (March-Diaz and Reyes, 2009). The SWR1 complex
110 associates extensively with chromatin and catalyzes H2A.Z exchange at genomic levels.

Consistently, SWR1-mediated chromatin remodeling is involved in diverse aspects of plant physiology and development, such as the floral transition, immune responses, and temperature sensing (Noh and Amasino, 2003; Deal et al., 2005; Kumar and Wigge, 2010). Here, we report that the EC associates with the SWR1 complex to repress the evening transcriptome. As a part of its biological impact, this complex shapes circadian oscillations by targeting clock genes such as *PRR7* and *PRR9* for H2A.Z deposition and gene repression. These results indicate that diurnal H2A.Z deposition provides a mechanism contributing to circadian gene expression in Arabidopsis.

Results

ELF3 stabilizes nucleosome architecture at EC target genes

To understand how the EC functions, we created a stringent list of direct EC targets (Supplemental Table S1), defined as genes whose promoters are bound by at least two EC proteins and which are mis-expressed at the end of the day in *elf3-1* (Ezer et al., 2017). Previously, we have seen that EC targets show the same pattern of mis-expression in both *elf3-1* and *lux-4*, when compared to wild type over a 24 h time course (Ezer et al., 2017). In both cases, there is minimal deviation from wild-type gene expression during the day, but maximal deviation during the evening and night-time, coinciding with the activity of the EC (Huang and Nusinow, 2016). Furthermore, the fold-increase in expression in *elf3-1* and *lux-4* is also conserved between target genes (Ezer et al., 2017). This indicates that the EC components control target gene expression possibly altogether. Thus, we next asked how the EC globally controls endogenous gene expression programs.

Since chromatin accessibility, which is related to gene responsiveness, is usually coordinated with transcriptional regulation, we investigated if EC targets have a distinctive

nucleosome structure, and if this is perturbed in *elf3-1*. Micrococcal nuclease (MNase) produces double-stranded cuts between nucleosomes, thus providing a simple method for obtaining information on the locations and arrangements of nucleosomes (Shu et al., 2013). We investigated the genome accessibility of the EC target loci at a range of time points using MNase digestion coupled with sequencing (MNase-seq). We observed high nucleosome occupancy for EC target genes (Fig. 1A-F), and this increased at ZT8 and ZT12 (Fig. 1B, C, E, and F), coinciding with maximal EC activity. Notably, a marked increase in chromatin accessibility was observed in the *elf3-1* mutant (Fig. 1B, C, E, and F), consistent with the EC repression of gene expression. The nucleosome occupancy in *elf3-1* was most similar to wild type at ZT0 (Fig. 1A and D), but decreased as the day progresses, showing the greatest loss at ZT12, by which time the gene body nucleosome occupancy was barely detectable (Fig. 1C and F). These results suggest that EC-dependent gene repression is induced in part by temporal stabilization of repressive chromatin structures.

Components of the SWR1 complex are necessary for EC function

To identify genes mediating the connection between the EC and chromatin architecture, we surveyed the DIURNAL dataset (http://diurnal.mocklerlab.org) for transcripts having a similar expression pattern to the EC. Transcripts encoding histone variants as well as SWR1 components required for H2A.Z deposition were included, and they were regulated in diurnal and circadian patterns (Supplemental Fig. S1A). To confirm these observations, we examined the circadian expression of genes associated with H2A.Z exchange by reverse transcription quantitative PCR (RT-qPCR) analysis. Genes encoding the SWR1 components, including *ARP6*, *PIE1*, and *SEF*, displayed circadian oscillation under free-running conditions with a peak around dusk (Fig. 2A-C), similar to *ELF3* (Fig. 2D). The transcript accumulation of

159 histone variant genes, *HTA8*, *HTA9*, and *HTA11*, however did not significantly oscillate during
160 the circadian cycle in our conditions (Supplemental Fig. S1B).

161 To determine if H2A.Z-nucleosomes are important for EC function, we analyzed
162 whether EC targets are mis-expressed in *arp6-1*, which is compromised in its ability to
163 incorporate H2A.Z-nucleosomes (Kumar and Wigge, 2010). Expression of EC target genes
164 over a diurnal cycle was analyzed using RNA-seq. These genes in this cluster showed a
165 pattern of increased expression at the end of day and early night in *arp6-1* compared to wild
166 type (Fig. 3A), a pattern consistent with reduced EC function in *arp6-1*.

167 Since warm temperature reduces the ability of the EC to associate with target
168 promoters (Box et al., 2015; Ezer et al., 2017), we investigated how these genes respond to
169 27ºC. As expected, EC targets were up-regulated in wild type at 27ºC particularly around
170 evening and night time (Fig. 3B), reflecting impaired EC function. This pattern was however
171 strongly enhanced by the *arp6-1* mutation (Fig. 3B). These results indicate that the EC and
172 H2A.Z-nucleosomes function to repress EC targets.

173

174 **ELF3 physically interacts with SEF**

175 Having established a connection between the EC-dependent gene repression and H2A.Z-
176 nucleosomes, we sought to investigate if there might be a direct physical interaction between
177 the components involved in these processes. To test this possibility, we performed yeast-two-
178 hybrid (Y2H) assays. Constructs of components of the SWR1 complex, ACTIN-RELATED
179 PROTEIN 4 (ARP4), ARP6, SEF, SWR COMPLEX PROTEIN 2 (SWC2) and SWC5, fused
180 with GAL4 DNA-binding domain (BD) and evening-expressed clock components fused with
181 GAL4 activation domain (AD) were co-expressed in yeast cells. Cell growth on selective
182 medium revealed that SEF interacts specifically with ELF3 (Fig. 4A and Supplemental Fig.

S2). Although ELF4 is also a member of the EC (Huang et al., 2016), we did not observe interactions of SEF with ELF4 in yeast cells (Fig. 4A). Since the PHOTOPERIOD-INDEPENDENT EARLY FLOWERING 1 (PIE1) protein is a catalytic core of SWR1 complex, we also examined interactions between PIE1 and EC components. We had difficulties cloning the full-length PIE1 and instead assayed domains of PIE1. Our results showed that the SANT domain of PIE1 was able to interact with ELF3 (Supplemental Fig. S3). Together, the results indicate that PIE1, possibly along with SEF, participate in the physical interactions with ELF3.

To confirm the physical interaction *in vivo*, we carried out bimolecular fluorescence complementation (BiFC) assays using Arabidopsis protoplasts. The *SEF* cDNA sequence was fused in-frame to the 5'-end of a gene sequence encoding the N-terminal half of YFP, and the *ELF3* gene was fused in-frame to the 5'-end of a sequence encoding the C-terminal half of YFP. The fusion constructs were then transiently co-expressed in Arabidopsis protoplasts. Strong yellow fluorescence was detected in the nucleus of cells co-expressing the combination of SEF-ELF3 (Fig. 4B), while co-expression with empty vectors did not show visible fluorescence (Fig. 4B). To quantify the physical interaction, split Luciferase (Luc) assay was also employed. ELF3 was fused with the amino part of Luc (NLuc), and SEF was fused with carboxyl-part of Luc (CLuc) (Fig. 4C). Co-expression of ELF3-NLuc and SEF-CLuc in Arabidopsis protoplasts resulted in 2-fold increase of Luc activity, while co-expression of controls showed background-level Luc activities (Fig. 4C). The *in planta* interactions of ELF3 and SEF were confirmed by coimmunoprecipitation (Co-IP) assays using *Nicotiana benthamiana* cells transiently coexpressing 35S:*ELF3-GFP* and 35S:*SEF-MYC* fusion constructs. Because the full-length ELF3 protein is a large protein, it is difficult to express transiently in *N. benthamiana*. As an alternative, we designed fragments of ELF3

fused with GFP and used them to test physical interactions with SEF (Fig. 4D). Co-IP analysis revealed that the C-terminal region of ELF3 was responsible for interactions with SEF *in planta* (Fig. 4D). These results indicate that the EC directly interacts with the SWR1 complex, and this may facilitate the direct deposition of H2A.Z-nucleosomes at EC target genes.

H2A.Z-nucleosomes are deposited at EC target loci

Since EC target genes are mis-regulated in *arp6-1* and ELF3 and SEF interact directly, we investigated if H2A.Z-nucleosomes are enriched at EC target genes. HTA11 occupancy, assayed by ChIP-seq (Cortijo et al., 2017), showed a strong enrichment across the gene body of ELF3 targets (Fig. 5A). The occupancy was particularly high at the region surrounding the TSS at the presumptive +1 nucleosome, but was also markedly higher over the gene body of ELF3 targets (Fig. 5A). By comparison, randomly selected control genes showed H2A.Z enrichment around the TSS only (Fig. 5B and Supplemental Table S2).

We then compared the genome-wide association of ELF3 with H2A.Z. Consistent with the fact that the EC is recruited to target sites via LUX binding sites and G-box motifs (Ezer et al., 2017), we observed that these motifs were strongly enriched at ELF3-binding sites (Ezer et al., 2017). Notably, the footprint bound by ELF3 in the promoters of EC target genes, including *PRR7, PRR9* and *LUX*, was devoid of H2A.Z-nucleosome signal (Fig. 5C and Supplemental Fig. S4A-C**)**, but the adjacent regions including the gene bodies were highly occupied with H2A.Z-nucleosomes (Fig. 5C and Supplemental Fig. S4A-C). This anti-phasing between H2A.Z occupancy and the EC was observed for all the EC targets (Fig. 5C and Supplemental Fig. S4A-C). H2A.Z-nucleosomes are refractory to transcription (Thakar et al., 2010), suggesting that the initial binding of the EC to the promoters of target genes may assist subsequent recruitment of H2A.Z-nucleosomes to repress EC target gene expression.

We thus further determined whether H2A.Z deposition is dependent on the EC. ChIP-seq assays showed that the H2A.Z occupancy was observed in EC-target genes particularly during night time (Fig. 5D and Supplemental Fig. S4D), whereas enrichment of H2A.Z-nucleosomes at those loci was compromised in the *elf3-1* mutant (Fig. 5E and Supplemental Fig. S4D). As a negative control, randomly selected control genes showed no temporal H2A.Z enrichment regardless of genetic background (Supplemental Fig. S4E). Further, we also obtained two additional lists of control genes: (1) genes bound by both ELF3 and LUX, but not up-regulated in *elf3-1* and *lux-4* mutants (Supplemental Table S3); (2) genes up-regulated in *elf3-1* and *lux-4*, but not bound by either ELF3 or LUX (Supplemental Table S4). Again, H2A.Z deposition was not diurnally regulated and influenced by ELF3 in both cases (Supplemental Figs. S5 and S6). These results indicate that the EC-SWR1 complex contributes to H2A.Z deposition at the EC target loci.

Temporal regulation of H2A.Z deposition at the *PRR7* and *PRR9* promoters underlies proper circadian oscillation

Given the essential role of the EC in the circadian clock and the direct physical and functional interaction between the EC and the SWR1 complex, SWR1 might be also important for proper circadian clock function. We used genetic mutants affected in the key SWR1 subunits, *arp6-1* and *sef-1*, and analyzed circadian function by monitoring the expression of a circadian output gene, *COLD, CIRCADIAN RHYTHM, AND RNA BINDING 2* (*CCR2*). RT-qPCR analysis revealed that the rhythmic amplitude of *CCR2* expression was significantly dampened in the two mutants (Supplemental Fig. S7). Similarly, the circadian expression of *CCR2* was also reduced in *hta9-1 hta11-2* double mutant (Supplemental Fig. S8), in a

254 comparable trend to that of SWR1 mutants. These results suggest that SWR1 activity and
255 proper circadian exchange of H2A.Z-nucleosomes might be important for circadian function.

256 Next we aimed to decipher the clock factors that are direct targets of the SWR1
257 complex. We thus employed *pHTA11:HTA11-GFP* transgenic plants and examined H2A.Z
258 deposition at core clock gene promoters by ChIP assays with a GFP-specific antibody. ChIP-
259 qPCR analysis showed that H2A.Z deposition specifically occurs at the gene bodies of the
260 morning-expressed genes *PRR7* and *PRR9* (Fig. 6A), whereas other core clock genes did not
261 show significant diurnal enrichment of the H2A.Z variant (Supplemental Fig. S9).
262 Furthermore, H2A.Z accumulation was primarily observed around dusk at the *PRR7* and
263 *PRR9* loci (Fig. 6A**)**, which is consistent with the temporal expression patterns of the ELF3
264 and SWR1 components (Fig. 2A-D).

265 We also generated transgenic plants over-expressing *SEF* (35S:*MYC-SEF*), in which
266 the core component of the SWR1 complex, SEF, is fused in-frame to 6 copies of MYC-coding
267 sequence. qPCR analysis following ChIP assays with an anti-MYC antibody showed that the
268 SWR1 component binds to the *PRR7* and *PRR9* loci (Fig. 6B). These results support the
269 specific association of SEF with the morning-expressed genes and agree with the pattern of
270 H2A.Z deposition. H2A.Z-nucleosome deposition usually inhibits Pol II accessibility by
271 stimulating closed chromatin formation (Kumar and Wigge, 2010). Consistent with this, Pol II
272 recruitment was significantly increased at *PRRs* in the *sef-1* mutant (Fig. 6C), which has
273 lower catalytic activity of H2A.Z deposition. These results indicate that H2A.Z deposition
274 occurs around dusk at EC target loci such as *PRR7* and *PRR9* to repress their expression.
275

276 **ELF3 is necessary for H2A.Z deposition at *PRR*s in the control of circadian oscillation**

The SEF-ELF3 direct interaction suggests that there may be functional coordination in the temporal regulation of *PRR7* and *PRR9*. To investigate this, we employed *pELF3::ELF3-MYC/elf3-1* and 35S:*MYC-ELF3* transgenic plants (Jang et al., 2015) and performed ChIP assays using an anti-MYC antibody. ChIP-qPCR analysis confirmed that ELF3 binds to the *PRR7* and *PRR9* loci (Fig. 7A), and this binding occurs preferentially at dusk (Supplemental Fig. S10). Consistent with the requirement of ELF4 and LUX in a functional EC, over-expression of *ELF3* still resulted in rhythmic binding.

Chromatin binding of ELF3 is causal for H2A.Z deposition and is independent of H2A.Z occupancy. We genetically crossed *pELF3::ELF3-MYC* transgenic plants with *arp6-1*, which lacks genome-wide H2A.Z deposition, and the *pELF3::ELF3-MYC x arp6-1* plants were used for ChIP assays using an anti-MYC antibody (Supplemental Fig. S11). As a result, ELF3 binding to *PRR* loci was comparable in both wild-type and *arp6-1* backgrounds (Supplemental Fig. S12), indicating that ELF3 binding is an active process to trigger H2A.Z deposition at cognate regions.

To determine the possible regulation of H2A.Z deposition by ELF3, we examined H2A.Z occupancy by ChIP-qPCR at *PRR7* and *PRR9* in *elf3-8*. As expected, H2A.Z deposition was reduced at these loci in *elf3-8*, particularly around dusk (Fig. 7B and Supplemental Fig. S13), indicating that ELF3 is both present on these promoters and facilitates the insertion or stability of repressive H2A.Z-nucleosomes (Fig. 7B). Consistently, binding of SEF was specifically observed at dusk, and its association to the *PRR7* and *PRR9* promoters occurred in an ELF3-dependent manner (Fig. 7C).

Consistent with the role of the EC and SWR1 complex in the repression of gene expression, the EC-SWR1 complex contributes to the declining phase of *PRR7* and *PRR9* expression during the evening and night period, when its expression is returning to basal

levels (Farre et al., 2005). As expected, Pol II accessibility of *PRR7* and *PRR9* was elevated at dusk in *elf3-8* (Fig. 7D). In further support of these results, expression of *PRR7* and *PRR9* was elevated during evening and night-time in *elf3-8* and H2A.Z-deficient *hta8 hta9 hta11* (*hta.z*) mutants (Fig. 7E). In addition, consistent with the repressing functions of PRR7 and PRR9 on *CCA1* and *LHY* (Nakamichi et al., 2010), expression of *CCA1* and *LHY* was significantly repressed during subjective morning in *elf3-8* and *hta.z* mutants (Supplemental Fig. S14). Clock-controlled *PHYTOCHROME-INTERACTING FACTOR 4* (*PIF4*) expression was also affected in *elf3-8* and *hta.z* mutants, and especially, its expression was derepressed during night period (Supplemental Fig. S14). To confirm the genetic interactions of EC and SWR1, we crossed *elf3-8* with 35S:*MYC-SEF* transgenic plants (Supplemental Fig. S15). 35S:*MYC-SEF* transgenic plants displayed repressed rhythmic expression of *PRR7* and *PRR9* compared with wild-type plants, whereas arrhythmic expression was observed in *elf3-8* (Fig. 7F). Notably, the 35S:*MYC-SEF/elf3-8* plants showed arrhythmicity similar to *elf3-8* (Fig. 7F), indicating that the SWR1 complex depends on the EC in the control of circadian oscillation.

In summary, the EC interaction with the SWR1 complex provides a mechanism to recruit transcriptionally repressive H2A.Z-nucleosomes at circadian regulated genes. In this way, targets may be repressed over the course of the night until the EC abundance declines and/or strong activation signals reactivate gene expression. In the case of circadian regulation, the *PRR7* and *PRR9* genes are under the temporal regulation of H2A.Z exchange. The EC-SWR1 complex is recruited to *PRR7* and *PRR9*, facilitating H2A.Z deposition to reduce gene expression during evening and night-time. This indicates a role for the EC in establishing circadian waves of gene expression.

Discussion

EC-dependent coordination of chromatin structures

The ELF3, ELF4, and LUX proteins form the tripartite EC complex and cooperatively regulate a variety of developmental processes. They are functionally intertwined in the gating of day-inducible genes (Hazen et al., 2005; Huang and Nusinow, 2016), and thus their genetic mutants share phenotypic alterations, such as elongated hypocotyls, early flowering, and altered circadian rhythms (Hicks et al., 2001; Hazen et al., 2005; Nusinow et al., 2011). Consistently, their binding sites largely overlap, and the EC controls target gene expression (Ezer et al., 2017). Here, we show that the EC recruits repressive chromatin domains to regulate the evening transcriptome. The EC interacts with the SWR1 complex and establishes transcriptionally-repressive H2A.Z-nucleosomes at its target genes. The high occupancy of H2A.Z-nucleosomes across the gene bodies of target genes provides an effective barrier to RNA Pol II, maintaining these genes in a repressed state.

Notably, mutants eliminating EC activity, like *elf3* and *lux*, exhibit an arrhythmic circadian clock. In contrast, SWR1 mutants are rhythmic but with reduced amplitude. Therefore, deposition of H2A.Z by the EC at core clock genes, such as *PRR7* and *PRR9*, is important for correct expression amplitude. However, circadian clock rhythmicity appears not to depend on this mechanism. Additionally, we cannot rule out the possibility that ELF3 may recruit additional chromatin modifiers and/or remodelers. The EC might be an important platform facilitating chromatin reconfiguration with multiple epigenetic modifications.

Temporal exchange of H2A.Z-nucleosomes provides a mechanism for diurnal gating of several physiological processes. For example, a majority of stress-responsive genes are gated primarily during day period (Seo and Mas, 2015), and consistently, a substantial number of stress-inducible genes that are responsive to drought, temperature, or pathogens are under the control of EC-dependent H2A.Z deposition in order to ensure their suppression during

night-time (Ezer et al., 2017). In addition, the circadian clock relies on a series of waves of transcriptional activation and repression. The recruitment of H2A.Z-nucleosomes provides a mechanism for the stable repression of target clock genes over the course of the night, which can be robustly activated the following day. Overall, the EC-SWR1 complex is a global transcriptional regulator that functions in the diurnal gating of many developmental and physiological processes and provides a more stable mechanism for maintaining repressive states during night-time.

Chromatin-based regulation at the core of the circadian clock

Time-of-day-dependent accumulation of chromatin marks such as H3ac and H3K4me3 occurs with the circadian transcript abundance of clock genes including *CCA1*, *LHY*, *TOC1*, *PRR7*, *PRR9*, and *LUX* (Hsu et al., 2013; Voss et al., 2015). Mechanistically, H3ac stimulates an open chromatin conformation (Song and Noh, 2012), whereas H3K4me3 inhibits the binding of clock repressor proteins to the core clock gene promoters, avoiding advanced circadian repressor binding (Malapeira et al., 2012). The SDG2/ATXR3 histone methyltransferase contributes to the H3K4me3 accumulation and thus controls the timing of clock gene expression, from activation to repression (Malapeira et al., 2012). Several additional chromatin modifiers, including HISTONE DEACETYLASE 6 (HDA6), HDA19, and JUMONJI C DOMAIN-CONTAINING PROTEIN 30/JUMONJI DOMAIN CONTAINING 5 (JMJ30/JMJD5), are also connected with the circadian oscillation (Jones and Harmer, 2011; Lu et al., 2011; Wang et al., 2013), although the mechanisms behind circadian gene regulation remain to be determined.

The epigenetic regulation of core clock genes relies on a complex web of chromatin and clock components. For example, CCA1 facilitates repressive chromatin signatures to

regulate *TOC1* expression around dawn while histone deacetylases contribute to the declining phase of *TOC1* (Perales and Mas, 2007). Another MYB-like transcription factor known as REVEILLE 8/LHY-CCA1-LIKE 5 (RVE8/LCL5) favors H3 acetylation at the *TOC1* promoter, most likely by antagonizing CCA1 function throughout the day (Farinas and Mas, 2011).

In this study, we identify a repressive chromatin state that shapes the rhythmic oscillations in gene expression. Circadian H2A.Z deposition underlies normal circadian oscillation, and *PRR7* and *PRR9* are primary targets of the SWR1 complex. H2A.Z-nucleosome deposition occurs around dusk, when the SWR1 components are highly expressed, to suppress gene expression. The interaction between the SWR1 complex and ELF3 provides a direct mechanism to facilitate H2A.Z exchange at cognate regions, contributing to precise oscillations in circadian gene expression. Since the *PRR7* and *PRR9* loci are also subjected to H3ac and H3K4me3 modifications (Malapeira et al., 2012), the higher-order combination of multiple chromatin modifications ultimately shapes the circadian waveforms of gene expression throughout the day-night cycle.

In mammals, rhythmical H2A.Z deposition at the promoters of CLOCK:BMAL1 targets has been observed, although the underlying mechanism is not known (Menet et al., 2014). This suggests that H2A.Z-nucleosomes may have a conserved function in the eukaryotic circadian clock.

Materials and Methods

Plant materials and growth conditions

Arabidopsis (*Arabidopsis thaliana*) (Columbia-0 ecotype) was used for all experiments unless otherwise specified. Arabidopsis seeds were surface sterilized and sown on 0.7% (w/v) agar

plates containing half strengthened Murashige and Skoog media. After 3-day stratification at 4°C, the seeds were grown in a Conviron reach-in chamber with 170 μmol m^{-2} s^{-1} light intensity and 70% humidity under short day (8 h light/16 h dark), neutral day (12 h light/12 h dark), or long day (16 h light/8 h dark) conditions at 22°C or 27°C, as indicated in figure legends. The *arp6-1*, *arp6-3*, *elf3-1*, *elf3-8*, *hta9-1hta11-2*, *pHTA11:HTA11-FLAG*, *pHTA11:HTA11-GFP*, and *sef-1* plants were previously reported (March-Diaz et al., 2007; Kumar and Wigge, 2010; Coleman-Derr and Zilberman, 2012; Rosa et al., 2013; Nitschke et al., 2016). To produce transgenic plants overexpressing the *SEF* and *ELF3* genes, a full-length cDNA was subcloned into the binary pBA002 vector under the control of the CaMV 35S promoter. *Agrobacterium tumefaciens*-mediated Arabidopsis transformation was then performed.

MNase-seq and ChIP-seq experiments and analysis

Approximately 1 g of 9-day-old Arabidopsis seedlings was harvested at the time points indicated in figure legends. The harvested seedlings were ground in liquid nitrogen to fine powder. The tissue powder was fixed for 10 min with 1% (v/v) formaldehyde (SIGMA, F8775) in Buffer 1 (0.4 M sucrose, 10 mM HEPES, 10 mM $MgCl_2$, 5 mM β-mercaptoethanol, 0.1 mM phenylmethylsulfonyl fluoride (PMSF) and 1 X protease inhibitor (Roche, 11836145001)). The reaction was quenched by adding glycine to a final concentration of 127 mM. The homogenate was filtered through Mira-cloth twice and centrifuged to collect the pellet. The pellet was washed in Buffer 2 (0.24 M sucrose, 10 mM Tris-HCl (pH 8.0), 10 mM $MgCl_2$, 5 mM β-mercaptoethanol, 0.1 mM PMSF and 1 X protease inhibitor, 1% v/v Triton) and then spun down in Buffer 3 (1.7 M sucrose, 10 mM Tris-HCl (pH 8.0), 10 mM $MgCl_2$, 5

mM β-mercaptoethanol, 0.1 mM PMSF and 1 X protease inhibitor, 0.15% v/v Triton). The nuclei pellet was then resuspended in Mnase Digestion Buffer (20 mM Tris-HCl (pH 8.0), 50 mM NaCl, 1 mM DTT, 0.5% (v/v) NP-40, 1 mM $CaCl_2$, 0.5 mM PMSF, 1 X protease inhibitor) and was flash frozen in liquid nitrogen twice to break the nuclear envelope. Chromatin was digested by adding Mnase (SIGMA, N3755) to a final concentration of 0.4 U/ml for 12.5 min. The reaction was terminated by adding EDTA to a final concentration of 5 mM. For ChIP-seq samples, H2A.Z in transgenic line *pHTA11:HTA11-FLAG* was immunoprecipitated by anti-FLAG M2 magnetic beads (SIGMA, M8823) and then eluted with 3XFLAG peptide (Bimake, B23112). After reverse crosslinking, the DNA was purified with SPRI beads. The libraries were constructed using TruSeq ChIP Sample Preparation Kit (Illumina, IP-202-1024) according to the manufacturer's instructions. The libraries were sequenced on an Illumina Nextseq 500 platform. The raw reads obtained from the sequencing facilities were analyzed using a combination of publicly available software and in-house scripts. We first assessed the quality of reads using FastQC:(www.bioinformatics.babraham.ac.uk/projects/fastqc/). Potential adaptor contamination and low quality trailing sequences were removed using Trimmomatic (Bolger et al., 2014). Then, the reads were mapped to the TAIR10 reference genome using Bowtie2 (Langmead and Salzberg, 2012). Duplicates were removed with the Picard tools (https://github.com/broadinstitute/ picard) and the read counts was normalised by the sample's genome-wide reads coverage. Nucleosome positioning and occupancy were determined using DANPOS (Chen et al., 2013). Nucleosome and H2A.Z average binding profiles and heatmaps were generated using deepTools (Ramirez et al., 2014).

442 The ‘randomly selected control genes’ were generated using ‘sample()’ function in R.
443 The indices of the 52 genes were generated by the R code ‘index <- sample(33557, 52)’,
444 where 33557 is the total number of Arabidopsis genes. The corresponding AGI gene names
445 were generated by the R code ‘random52 <- all_gene_names[index,]’. In addition, we also
446 obtained two additional lists of control genes with new filters: 1) genes bound by both ELF3
447 and LUX, but not up-regulated in *elf3-1* and *lux-4* mutants (Supplemental Table S3), and 2)
448 genes up-regulated in *elf3-1* and *lux-4*, but not bound by either ELF3 or LUX (Supplemental
449 Table S4). The filter criteria for the former gene list are: A) having both ELF3 and LUX
450 binding within 1000 bp upstream of the gene; and B) the log fold changes of TPM values
451 compared with Col-0 at ZT16 are smaller than 0.5-fold in both *elf3-1* and *lux-4* mutants. The
452 filter criteria for the latter gene list are : A) having no ELF3 or LUX binding within 1000 bp
453 upstream of the gene; and B) the log fold changes of TPM values compared with Col-0 at
454 ZT16 are larger than 1.5-fold in both *elf3-1* and *lux-4* mutants.
455
456 **RNA-seq experiment and analysis**
457 Approximately 30 mg of 7-day-old Arabidopsis seedlings were harvested and their total RNA
458 was extracted using the MagMAX-96 Total RNA Isolation kit (Ambion, AM1830) according
459 to manufacturer’s instructions. Library preparation was performed using 1 μg of high integrity
460 total RNA (RIN>8) using the TruSeq Stranded mRNA library preparation kit (Illumina, RS-
461 122-2103) according to the manufacturer’s instructions. The libraries were sequenced on an
462 Illumina Nextseq 500 platform.
463 For bioinformatics analysis, we first assessed the quality of reads using FastQC:
464 (www.bioinformatics.babraham.ac.uk/projects/fastqc/). Potential adaptor contamination and
465 low quality trailing sequences were removed using Trimmomatic (Bolger et al., 2014), before

alignment to the TAIR10 transcriptome using Tophat (Trapnell et al., 2009). Potential optical duplicates resulting from library preparation were removed using the Picard tools (https://github.com/broadinstitute/picard), and the read counts were normalized by the sample's genome-wide reads coverage. Raw counts were determined by HTseq-count (Anders et al., 2015), and cufflinks was utilized to calculate Fragments Per Kilobase Million (FPKM), which was then converted into Transcripts Per Million (TPM).

Reverse transcription quantitative PCR (RT-qPCR) analysis

Total RNA was extracted using TRI reagent (TAKARA Bio, Singa, Japan) according to the manufacturer's recommendations. Reverse transcription (RT) was performed using Moloney Murine Leukemia Virus (M-MLV) reverse transcriptase (Dr. Protein, Seoul, South Korea) with oligo(dT18) to synthesize first-strand cDNA from 2 μg of total RNA. Total RNA samples were pretreated with an RNAse-free DNAse. cDNAs were diluted to 100 μL with TE buffer, and 1 μL of diluted cDNA was used for PCR amplification.

RT-qPCR reactions were performed in 96-well blocks using the Step-One Plus Real-Time PCR System (Applied Biosystems). The PCR primers used are listed in Supplemental Table S5. The values for each set of primers were normalized relative to the *EUKARYOTIC TRANSLATION INITIATION FACTOR 4A1* (*eIF4A*) gene (At3g13920). All RT-qPCR reactions were performed with biological triplicates using total RNA samples extracted from three independent replicate samples. The comparative ΔΔCT method was employed to evaluate relative quantities of each amplified product in the samples. The threshold cycle (CT) was automatically determined for each reaction with the analysis software set using

default parameters. The specificity of the RT-qPCR reactions was determined by melting curve analysis of the amplified products using the standard method employed by the software.

Yeast two-hybrid assays

Yeast two-hybrid (Y2H) assays were performed using the BD Matchmaker system (Clontech, Mountain View, CA, USA). The pGADT7 vector was used for the GAL4 AD fusion, and the pGBKT7 vector was used for GAL4 BD fusion. The yeast strain AH109 harboring the LacZ and His reporter genes was used. PCR products were subcloned into the pGBKT7 and pGADT7 vectors. The expression constructs were co-transformed into yeast AH109 cells and transformed cells were selected by growth on SD/-Leu/-Trp medium and SD/-Leu/-Trp/-His/-Ade. Interactions between proteins were analyzed by measuring β-galactosidase (β-Gal) activity using o-nitrophenyl-β-D-galactopyranoside (ONPG) as a substrate.

Bimolecular fluorescence complementation (BiFC) assays

The *ELF3* gene was fused in-frame to the 5′ end of a gene sequence encoding the C-terminal half of EYFP in the pSATN-cEYFP-C1 vector (E3082). The *SEF* cDNA sequence was fused in-frame to the 5′ end of a gene sequence encoding the N-terminal half of EYFP in the pSATN-nEYFP-C1 vector (E3081). Expression constructs were co-transformed into Arabidopsis protoplasts. Expression of the fusion constructs was monitored by fluorescence microscopy using a Zeiss LSM510 confocal microscope (Carl Zeiss, Jena, Germany).

Chromatin immunoprecipitation (ChIP) assays

The epitope-tagged transgenic plant samples were cross-linked with 1% (v/v) formaldehyde, ground to powder in liquid nitrogen, and then sonicated. The sonicated chromatin complexes

were bound with corresponding antibodies. Anti-MYC (05-724, Millipore, Billerica, USA), anti-Pol II (sc-33754, Santa Cruz, Dallas, Texas, USA), anti-H2A.Z antibodies (ab4174, Abcam, Cambridge, UK), and salmon sperm DNA/protein A agarose beads (16-157, Millipore, Billerica, USA) were used for chromatin immunoprecipitation. DNA was purified using phenol/chloroform/isoamyl alcohol and sodium acetate (pH 5.2). The level of precipitated DNA fragments was quantified by quantitative PCR (qPCR) using specific primer sets (Supplemental Table S6). Values were normalized according to input DNA levels. Values for control plants were set to 1 after normalization against *eIF4a* for qPCR analysis.

Split-luciferase assays

The coding regions of *SEF* and *ELF3* were cloned into pcFLucC or pcFLucN vector. The recombinant constructs were cotransformed with into Arabidopsis protoplasts by polyethylene glycol–mediated transformation. The *pUBQ10::GUS* plasmid was also cotransformed as an internal control to normalize the LUC activity.

Coimmunoprecipitation (Co-IP) assays

Agrobacterium tumefaciens cells containing 35S:*SEF-MYC* and 35S:*ELF3-GFP* constructs were infiltrated to 3-week-old *Nicotiana benthamiana* leaves. *N. benthamiana* leaves were homogenized in protein extraction buffer (25 mM Tris-HCl, pH 7.5, 150 mM NaCl, 5% v/v glycerol, 0.05% w/v Nonidet P-40, 2.5 mM EDTA, 1 mM phenylmethylsulfonyl fluoride, and 1 × complete cocktail of protease inhibitors). After protein extraction, anti-MYC antibodies (05-724, Millipore, Billerica, MA, USA) coupled to Protein-A sepharose beads (Sigma-Aldrich, St Louis, MO, USA) were mixed and incubated for 4 h at 4 °C. The precipitated samples were washed at least four times with the protein extraction buffer and then eluted by

1 × SDS–polyacrylamide gel electrophoresis (PAGE) loading buffer to perform SDS–PAGE with anti-MYC (1:2000 dilution; Millipore) or anti-GFP antibodies (1:1,000 dilution; sc-9996, Santa Cruz Biotech., Dallas, Texas, USA).

Statistical analysis

Unless otherwise specified, quantitative data are presented as mean ± SD and significance was assessed by the two-tailed Student's *t* test.

Accession numbers

The raw sequencing data reported in this work have been deposited in the NCBI Gene Expression Omnibus under accession number GSE109101.

Supplemental Data

The following supplemental materials are available in the online version of this article.

Supplemental Figure S1. Diurnal expression of H2A.Z-related genes.

Supplemental Figure S2. Yeast-two-hybrid assays.

Supplemental Figure S3. Interaction of ELF3 with PIE1.

Supplemental Figure S4. H2A.Z occupancy on EC-target genes.

Supplemental Figure S5. H2A.Z enrichment at genes bound by both ELF3 and LUX, but not differentially expressed in *elf3-1* and *lux-4* mutants.

Supplemental Figure S6. H2A.Z enrichment at genes up-regulated in *elf3-1* and *lux-4*, but not bound by either ELF3 or LUX.

Supplemental Figure S7. Reduced rhythmic amplitude in genetic mutants of SWR1 components.

Supplemental Figure S8. Influences on circadian clock in *hta9-1hta11-2*.

Supplemental Figure S9. Deposition of H2A.Z at clock gene promoters.

Supplemental Figure S10. Binding of ELF3 to the *PRR7* and *PRR9* promoters at ZT12.

Supplemental Figure S11. Protein accumulation of ELF3 in *pELF3::ELF3-MYC* and *pELF3::ELF3-MYCxarp6-1*.

Supplemental Figure S12. ELF3 binding to the *PRR* loci in *arp6-1* background.

Supplemental Figure S13. H2A.Z deposition in *elf3-8* mutant throughout a day.

Supplemental Figure S14. Expression of *CCA1*, *LHY*, and *PIF4* in *h2a.z* and *elf3-8* mutants.

Supplemental Figure S15. Protein accumulation of SEF in 35S:*MYC-SEF* and 35S:*MYC-SEFxelf3-8*.

Supplemental Table S1. EC target gene list.

Supplemental Table S2. 52 Randomly selected control genes.

Supplemental Table S3. List of genes bound by both ELF3 and LUX, but not differentially expressed in *elf3-1* and *lux-4* mutants.

Supplemental Table S4. List of genes up-regulated in *elf3-1* and *lux-4*, but not bound by either ELF3 or LUX.

Supplemental Table S5. Primers used in RT-qPCR analysis.

Supplemental Table S6. Primers used in ChIP assays.

Acknowledgements: We thank Dr. Hui Lan for bioinformatics data analysis. This work was supported by the Basic Science Research (NRF-2019R1A2C2006915) and Basic Research Laboratory (NRF-2017R1A4A1015620) programs provided by the National Research Foundation of Korea and by the Next-Generation BioGreen 21 Program (PJ01314501) provided by the Rural Development Administration to P.J.S. P.M. laboratory is funded by the

584 FEDER/Spanish Ministry of Economy and Competitiveness, by the Ramon Areces
585 Foundation and by the Generalitat de Catalunya (AGAUR). P.M. laboratory also
586 acknowledges financial support from the CERCA Program/Generalitat de Catalunya and by
587 the Spanish Ministry of Economy and Competitiveness through the "Severo Ochoa Program
588 for Centers of Excellence in R&D" 2016–2019 (SEV-2015-0533). Work in the lab of P.A.W.
589 is supported by the Gatsby Foundation (GAT3273/GLB).
590
591
592 **Conflict of interest**
593 The authors declare that they have no conflict of interest.
594
595 **Figure legends**
596 **Figure 1. Nucleosome occupancy in Evening Complex (EC) target genes in Col-0 and**
597 ***elf3-1* at ZT0, 8, and 12.**
598 Average nucleosome signals (normalized Mnase-seq reads) on 52 EC target genes (see also
599 Supplemental Table S1) at Zeitgeber Time 0 (ZT0), ZT8, and ZT12 (**A-C**) in Col-0 and *elf3-1*
600 grown under long day conditions (LD). Heat map visualization of nucleosome signals over 52
601 EC target genes on Col-0 and *elf3-1* at ZT0, ZT8, and ZT12 (**D-F**). Data are plotted from 1kb
602 upstream of TSS to 1kb downstream of TES of EC target genes. Graphs show the results of
603 two replicates. TSS: Transcription Start Site; TES: Transcription End Site.
604
605 **Figure 2. Coexpression of the SWR1 components with EC.**
606 **A-D** Circadian expression of SWR1 components and *ELF3*. Seedlings grown under neutral
607 day conditions (ND, 12h light: 12h dark) for 2 weeks were transferred to continuous light

conditions (LL) at Zeitgeber Time 0 (ZT0). Whole seedlings were harvested from ZT24 to ZT68 to analyze transcript accumulation. Transcript levels of *ARP6* (**A**), *PIE1* (**B**), *SEF* (**C**), and *ELF3* (**D**) were determined by reverse transcription quantitative PCR (RT-qPCR). Gene expression values were normalized to the *EUKARYOTIC TRANSLATION INITIATION FACTOR 4A1* (*eIF4A*) expression. Biological triplicates were averaged. Bars represent the standard error of the mean. The white and grey boxes indicate the subjective day and night, respectively.

Figure 3. Elevated expression of EC target genes in *arp6-1*.

Heat map visualization of log fold changes of the expression levels of EC target genes in *arp6-1* at 22ºC compared with Col-0 at 22ºC grown under LDs (**A**) and in *arp6-1* at 27ºC compared with Col-0 at 22ºC grown under short days (SDs) (**B**). Values in (**A**) and (**B**) represent $\log_2$ (TPM in *arp6-1* 22ºC / TMP in Col-0 22ºC) and $\log_2$ (TPM in *arp6-1* 27ºC / TMP in Col-0 22ºC), respectively. The log fold change of the expression level of each gene was calculated by Z-score (mean = 0, standard deviation = 1). The heat map was generated using heatmap.2 function in R (version 3.2.5).

Figure 4. Interactions of the SWR1 complex with EC.

A yeast-two-hybrid (Y2H) assays. Y2H assays were performed with the SEF protein fused to the DNA-binding domain (BD) of GAL4 and evening-expressed clock components fused with the transcriptional activation domain (AD) of GAL4 for analysis of interactions. Interactions were examined by cell growth on selective media. -LWHA indicates Leu, Trp, His, and Ade drop-out plates. -LW indicates Leu and Trp drop-out plates. GAL4 was used as a positive control (P).

B BiFC assays. Partial fragments of YFP protein were fused with SEF and ELF3, and co-expressed in Arabidopsis protoplasts. Reconstituted fluorescence was examined by confocal microscopy. IDD14-RFP was used as a nucleus marker. Bars: 10 μm.

C Interaction of ELF3-NLuc with SEF-CLuc. Partial fragments of Luciferase (NLuc and CLuc) were fused with ELF3 or SEF. The fusion constructs were coexpressed in Arabidopsis protoplasts and Luc activities were measured and normalized against total protein. Three independent biological replicates were averaged and statistically analyzed with Student's *t*-test (*$P < 0.05$). Bars indicate the standard error of the mean.

D Co-IP assays. *Agrobacterium tumefaciens* cells containing 35S:*ELF3*$^{N(1\text{-}345aa)}$*-GFP*, 35S:*ELF3*$^{C(346\text{-}695aa)}$*-GFP*, and 35S:*SEF-MYC* constructs were coinfiltrated to 3-week-old *N. benthamiana* leaves. Epitope-tagged proteins were detected immunologically using corresponding antibodies.

Figure 5. ELF3 and H2A.Z occupancy of EC target genes.

A, B H2A.Z enrichment (normalized HTA11-FLAG ChIP-seq reads) on 52 EC target genes (**A**) and control genes (**B**) was analyzed. For the class of 'control genes', a sample of 52 genes was randomly selected to compare their H2A.Z occupancy with EC target genes (see also Supplemental Table S2). (**A**) and (**B**) are plotted from 1kb upstream of the TSS to 1kb downstream of the TES of the corresponding genes.

C ELF3 and H2A.Z average binding plot on 52 EC target genes.

D, E H2A.Z enrichment in wild type (**D**) and *elf3-1* mutant (**E**) at various time points under LD conditions.

Figure 6. H2A.Z deposition at *PRR7* and *PRR9* loci by the SWR1 complex.

In (**A**) to (**C**), fragmented DNA was eluted from the protein-DNA complexes and used for qPCR analysis. Enrichment was normalized relative to *eIF4A*. Three independent biological replicates were averaged, and the statistical significance of the measurements was determined. Bars indicate the standard error of the mean.

A Accumulation of H2A.Z at clock gene loci. Two-week-old plants grown under ND were used for ChIP analysis with anti-GFP antibody. Gene structures are presented (upper panel). Underbars represent the amplified genomic regions. Statistically significant differences between ZT0 and ZT12 samples are indicated by asterisks (Student's *t*-test, $*P < 0.05$, $**P < 0.01$).

B Binding of SEF to clock gene promoters. Two-week-old 35S:*MYC-SEF* transgenic plants grown under ND were harvested at ZT12. Statistically significant differences between wild-type and 35S:*MYC-SEF* plants are indicated by asterisks (Student's *t*-test, $*P < 0.05$).

C Recruitment of Pol II at *PRR*s in *sef-1*. Two-week-old plants grown under ND were harvested at ZT12 and used for ChIP analysis with an anti-N-terminus of Arabidopsis Pol II antibody. qPCR was performed with a primer pair amplifying B region of each gene promoter (see also **Fig. 6A**). Statistically significant differences between WT and *sef-1* plants are indicated by asterisks (Student's *t*-test, $*P < 0.05$).

Figure 7. H2A.Z exchange at *PRR7* and *PRR9* loci by ELF3.

A Binding of ELF3 to *PRR* promoters. Two-week-old *pELF3::ELF3-MYC/elf3-1* seedlings grown under ND were harvested at ZT12 and used to conduct ChIP assays. Statistically significant differences between Col-0 and *pELF3::ELF3-MYC/elf3-1* plants are indicated by asterisks (Student's *t*-test, $*P < 0.05$, $***P < 0.001$).

B H2A.Z deposition at clock gene promoters in *elf3-8*. Two-week-old plants grown under ND were used for ChIP analysis with anti-H2A.Z antibody. Statistically significant differences between Col-0 and *elf3-8* plants are indicated by asterisks (Student's *t*-test, $*P < 0.05$, $***P < 0.001$).

C SEF binding to the *PRR* loci in *elf3-8* background. Two-week-old plants grown under ND were used for ChIP analysis with anti-MYC antibody. Statistically significant differences between ZT0 and ZT12 samples are indicated by asterisks (Student's *t*-test, $*P < 0.05$).

D Recruitment of Pol II at clock gene promoters in *elf3-8*. Two-week-old plants grown under ND were harvested at ZT12 and used for ChIP analysis with an anti-N-terminus of Arabidopsis Pol II antibody. In (**A**) to (**D**), fragmented DNA was eluted from the protein-DNA complexes and used for qPCR analysis. Enrichment was normalized relative to *eIF4A*. Three independent biological replicates were averaged, and the statistical significance of the measurements was determined by Student's *t*-test ($*P < 0.05$). Bars indicate the standard error of the mean.

E Circadian expression of *PRR7* and *PRR9* in *elf3-8* and *h2a.z*.

F *PRR* expression in 35S:*MYC-SEF/elf3-8*. In (**E**) and (**F**), seedlings grown under ND conditions for 2 weeks were transferred to LL at ZT0.

LITERATURE CITED

Alabadi D, Oyama T, Yanovsky MJ, Harmon FG, Mas P, Kay SA (2001) Reciprocal regulation between TOC1 and LHY/CCA1 within the Arabidopsis circadian clock. Science **293:** 880-883

Anders S, Pyl PT, Huber W (2015) HTSeq--a Python framework to work with high-throughput sequencing data. Bioinformatics **31:** 166-169

Bolger AM, Lohse M, Usadel B (2014) Trimmomatic: a flexible trimmer for Illumina sequence data. Bioinformatics **30:** 2114-2120

Box MS, Huang BE, Domijan M, Jaeger KE, Khattak AK, Yoo SJ, Sedivy EL, Jones DM, Hearn TJ, Webb AA, Grant A, Locke JC, Wigge PA (2015) ELF3 controls thermoresponsive growth in Arabidopsis. Curr Biol **25:** 194-199

Carre IA, Kim JY (2002) MYB transcription factors in the Arabidopsis circadian clock. J Exp Bot **53:** 1551-1557

Chen K, Xi Y, Pan X, Li Z, Kaestner K, Tyler J, Dent S, He X, Li W (2013) DANPOS: dynamic analysis of nucleosome position and occupancy by sequencing. Genome Res **23:** 341-351

Chow BY, Helfer A, Nusinow DA, Kay SA (2012) ELF3 recruitment to the PRR9 promoter requires other Evening Complex members in the Arabidopsis circadian clock. Plant Signal Behav **7:** 170-173

Coleman-Derr D, Zilberman D (2012) Deposition of histone variant H2A.Z within gene bodies regulates responsive genes. PLoS Genet **8:** e1002988

Cortijo S, Charoensawan V, Brestovitsky A, Buning R, Ravarani C, Rhodes D, van Noort J, Jaeger KE, Wigge PA (2017) Transcriptional Regulation of the Ambient Temperature Response by H2A.Z Nucleosomes and HSF1 Transcription Factors in Arabidopsis. Mol Plant **10:** 1258-1273

Deal RB, Kandasamy MK, McKinney EC, Meagher RB (2005) The nuclear actin-related protein ARP6 is a pleiotropic developmental regulator required for the maintenance of FLOWERING LOCUS C expression and repression of flowering in Arabidopsis. Plant Cell **17:** 2633-2646

Deal RB, Topp CN, McKinney EC, Meagher RB (2007) Repression of flowering in Arabidopsis requires activation of FLOWERING LOCUS C expression by the histone variant H2A.Z. Plant Cell **19:** 74-83

Ezer D, Jung JH, Lan H, Biswas S, Gregoire L, Box MS, Charoensawan V, Cortijo S, Lai X, Stockle D, Zubieta C, Jaeger KE, Wigge PA (2017) The evening complex coordinates environmental and endogenous signals in Arabidopsis. Nat. Plants **3:** 17087

Farinas B, Mas P (2011) Functional implication of the MYB transcription factor RVE8/LCL5 in the circadian control of histone acetylation. Plant J **66:** 318-329

Farre EM, Harmer SL, Harmon FG, Yanovsky MJ, Kay SA (2005) Overlapping and distinct roles of PRR7 and PRR9 in the Arabidopsis circadian clock. Curr Biol **15:** 47-54

Gendron JM, Pruneda-Paz JL, Doherty CJ, Gross AM, Kang SE, Kay SA (2012) Arabidopsis circadian clock protein, TOC1, is a DNA-binding transcription factor. Proc Natl Acad Sci U S A **109:** 3167-3172

Greenham K, McClung CR (2015) Integrating circadian dynamics with physiological processes in plants. Nat

733 Rev Genet **16:** 598-610
734 **Guillemette B, Bataille AR, Gevry N, Adam M, Blanchette M, Robert F, Gaudreau L** (2005) Variant histone
735 H2A.Z is globally localized to the promoters of inactive yeast genes and regulates nucleosome
736 positioning. PLoS Biol **3:** e384
737 **Hazen SP, Schultz TF, Pruneda-Paz JL, Borevitz JO, Ecker JR, Kay SA** (2005) LUX ARRHYTHMO
738 encodes a Myb domain protein essential for circadian rhythms. Proc Natl Acad Sci U S A **102:** 10387-
739 10392
740 **Herrero E, Kolmos E, Bujdoso N, Yuan Y, Wang M, Berns MC, Uhlworm H, Coupland G, Saini R,**
741 **Jaskolski M, Webb A, Goncalves J, Davis SJ** (2012) EARLY FLOWERING4 recruitment of EARLY
742 FLOWERING3 in the nucleus sustains the Arabidopsis circadian clock. Plant Cell **24:** 428-443
743 **Hicks KA, Albertson TM, Wagner DR** (2001) EARLY FLOWERING3 encodes a novel protein that regulates
744 circadian clock function and flowering in Arabidopsis. Plant Cell **13:** 1281-1292
745 **Hicks KA, Millar AJ, Carre IA, Somers DE, Straume M, Meeks-Wagner DR, Kay SA** (1996) Conditional
746 circadian dysfunction of the Arabidopsis early-flowering 3 mutant. Science **274:** 790-792
747 **Hsu PY, Devisetty UK, Harmer SL** (2013) Accurate timekeeping is controlled by a cycling activator in
748 Arabidopsis. Elife **2:** e00473
749 **Huang H, Alvarez S, Bindbeutel R, Shen Z, Naldrett MJ, Evans BS, Briggs SP, Hicks LM, Kay SA,**
750 **Nusinow DA** (2016) Identification of Evening Complex Associated Proteins in Arabidopsis by Affinity
751 Purification and Mass Spectrometry. Mol Cell Proteomics **15:** 201-217
752 **Huang H, Nusinow DA** (2016) Into the Evening: Complex Interactions in the Arabidopsis Circadian Clock.
753 Trends Genet **32:** 674-686
754 **Huang W, Perez-Garcia P, Pokhilko A, Millar AJ, Antoshechkin I, Riechmann JL, Mas P** (2012) Mapping
755 the core of the Arabidopsis circadian clock defines the network structure of the oscillator. Science **336:**
756 75-79
757 **Jang K, Lee HG, Jung SJ, Paek NC, Seo PJ** (2015) The E3 Ubiquitin Ligase COP1 Regulates Thermosensory
758 Flowering by Triggering GI Degradation in Arabidopsis. Sci Rep **5:** 12071
759 **Jones MA, Harmer S** (2011) JMJD5 Functions in concert with TOC1 in the arabidopsis circadian system. Plant
760 Signal Behav **6:** 445-448
761 **Kumar SV, Wigge PA** (2010) H2A.Z-containing nucleosomes mediate the thermosensory response in

762 Arabidopsis. Cell **140:** 136-147

763 **Langmead B, Salzberg SL** (2012) Fast gapped-read alignment with Bowtie 2. Nat Methods **9:** 357-359

764 **Lu SX, Knowles SM, Webb CJ, Celaya RB, Cha C, Siu JP, Tobin EM** (2011) The Jumonji C domain-
765 containing protein JMJ30 regulates period length in the Arabidopsis circadian clock. Plant Physiol **155:**
766 906-915

767 **Lu SX, Webb CJ, Knowles SM, Kim SH, Wang Z, Tobin EM** (2012) CCA1 and ELF3 Interact in the control
768 of hypocotyl length and flowering time in Arabidopsis. Plant Physiol **158:** 1079-1088

769 **Malapeira J, Khaitova LC, Mas P** (2012) Ordered changes in histone modifications at the core of the
770 Arabidopsis circadian clock. Proc Natl Acad Sci U S A **109:** 21540-21545

771 **March-Diaz R, Garcia-Dominguez M, Florencio FJ, Reyes JC** (2007) SEF, a new protein required for
772 flowering repression in Arabidopsis, interacts with PIE1 and ARP6. Plant Physiol **143:** 893-901

773 **March-Diaz R, Reyes JC** (2009) The beauty of being a variant: H2A.Z and the SWR1 complex in plants. Mol
774 Plant **2:** 565-577

775 **Menet JS, Pescatore S, Rosbash M** (2014) CLOCK:BMAL1 is a pioneer-like transcription factor. Genes Dev
776 **28:** 8-13

777 **Nakamichi N, Kiba T, Henriques R, Mizuno T, Chua NH, Sakakibara H** (2010) PSEUDO-RESPONSE
778 REGULATORS 9, 7, and 5 are transcriptional repressors in the Arabidopsis circadian clock. Plant Cell
779 **22:** 594-605

780 **Nitschke S, Cortleven A, Iven T, Feussner I, Havaux M, Riefler M, Schmulling T** (2016) Circadian Stress
781 Regimes Affect the Circadian Clock and Cause Jasmonic Acid-Dependent Cell Death in Cytokinin-
782 Deficient Arabidopsis Plants. Plant Cell **28:** 1616-1639

783 **Noh YS, Amasino RM** (2003) PIE1, an ISWI family gene, is required for FLC activation and floral repression
784 in Arabidopsis. Plant Cell **15:** 1671-1682

785 **Nusinow DA, Helfer A, Hamilton EE, King JJ, Imaizumi T, Schultz TF, Farre EM, Kay SA** (2011) The
786 ELF4-ELF3-LUX complex links the circadian clock to diurnal control of hypocotyl growth. Nature **475:**
787 398-402

788 **Perales M, Mas P** (2007) A functional link between rhythmic changes in chromatin structure and the
789 Arabidopsis biological clock. Plant Cell **19:** 2111-2123

790 **Pokhilko A, Mas P, Millar AJ** (2013) Modelling the widespread effects of TOC1 signalling on the plant

circadian clock and its outputs. BMC Syst Biol **7:** 23

Raisner RM, Hartley PD, Meneghini MD, Bao MZ, Liu CL, Schreiber SL, Rando OJ, Madhani HD (2005) Histone variant H2A.Z marks the 5' ends of both active and inactive genes in euchromatin. Cell **123:** 233-248

Raisner RM, Madhani HD (2006) Patterning chromatin: form and function for H2A.Z variant nucleosomes. Curr Opin Genet Dev **16:** 119-124

Ramirez F, Dundar F, Diehl S, Gruning BA, Manke T (2014) deepTools: a flexible platform for exploring deep-sequencing data. Nucleic Acids Res **42:** W187-191

Rangasamy D, Berven L, Ridgway P, Tremethick DJ (2003) Pericentric heterochromatin becomes enriched with H2A.Z during early mammalian development. EMBO J **22:** 1599-1607

Rosa M, Von Harder M, Cigliano RA, Schlogelhofer P, Mittelsten Scheid O (2013) The Arabidopsis SWR1 chromatin-remodeling complex is important for DNA repair, somatic recombination, and meiosis. Plant Cell **25:** 1990-2001

Salome PA, McClung CR (2004) The Arabidopsis thaliana clock. J Biol Rhythms **19:** 425-435

Salome PA, Weigel D, McClung CR (2010) The role of the Arabidopsis morning loop components CCA1, LHY, PRR7, and PRR9 in temperature compensation. Plant Cell **22:** 3650-3661

Seo PJ, Mas P (2014) Multiple layers of posttranslational regulation refine circadian clock activity in Arabidopsis. Plant Cell **26:** 79-87

Seo PJ, Mas P (2015) STRESSing the role of the plant circadian clock. Trends Plant Sci **20:** 230-237

Shu H, Gruissem W, Hennig L (2013) Measuring Arabidopsis chromatin accessibility using DNase I-polymerase chain reaction and DNase I-chip assays. Plant Physiol **162:** 1794-1801

Song HR, Noh YS (2012) Rhythmic oscillation of histone acetylation and methylation at the Arabidopsis central clock loci. Mol Cells **34:** 279-287

Staiger D, Green R (2011) RNA-based regulation in the plant circadian clock. Trends Plant Sci **16:** 517-523

Swaminathan J, Baxter EM, Corces VG (2005) The role of histone H2Av variant replacement and histone H4 acetylation in the establishment of Drosophila heterochromatin. Genes Dev **19:** 65-76

Thakar A, Gupta P, McAllister WT, Zlatanova J (2010) Histone variant H2A.Z inhibits transcription in reconstituted nucleosomes. Biochemistry **49:** 4018-4026

To TK, Kim JM (2014) Epigenetic regulation of gene responsiveness in Arabidopsis. Front Plant Sci **4:** 548

Trapnell C, Pachter L, Salzberg SL (2009) TopHat: discovering splice junctions with RNA-Seq. Bioinformatics **25:** 1105-1111

Voss U, Wilson MH, Kenobi K, Gould PD, Robertson FC, Peer WA, Lucas M, Swarup K, Casimiro I, Holman TJ, Wells DM, Peret B, Goh T, Fukaki H, Hodgman TC, Laplaze L, Halliday KJ, Ljung K, Murphy AS, Hall AJ, Webb AA, Bennett MJ (2015) The circadian clock rephases during lateral root organ initiation in Arabidopsis thaliana. Nat Commun **6:** 7641

Wang L, Kim J, Somers DE (2013) Transcriptional corepressor TOPLESS complexes with pseudoresponse regulator proteins and histone deacetylases to regulate circadian transcription. Proc Natl Acad Sci U S A **110:** 761-766

Yerushalmi S, Yakir E, Green RM (2011) Circadian clocks and adaptation in Arabidopsis. Mol Ecol **20:** 1155-1165

Figure 1

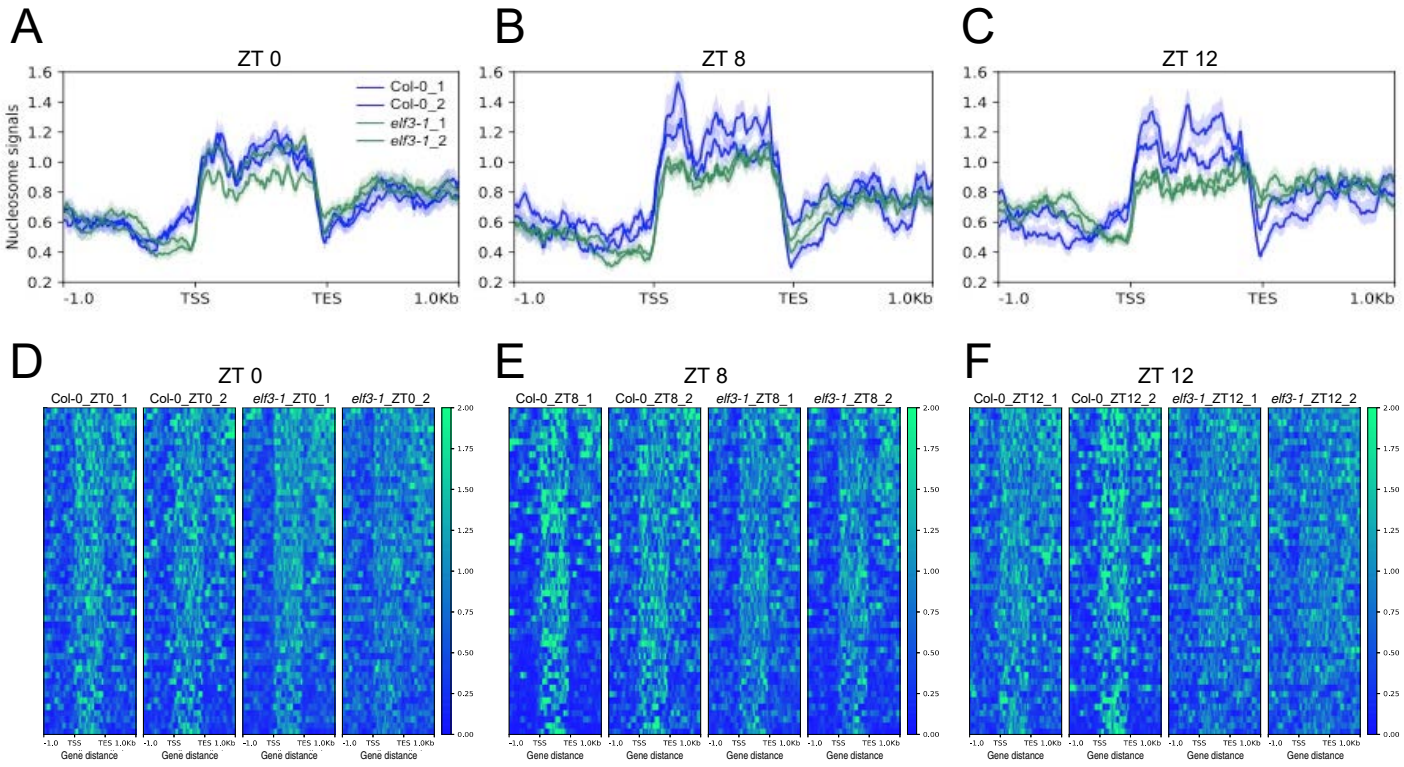

Figure 2

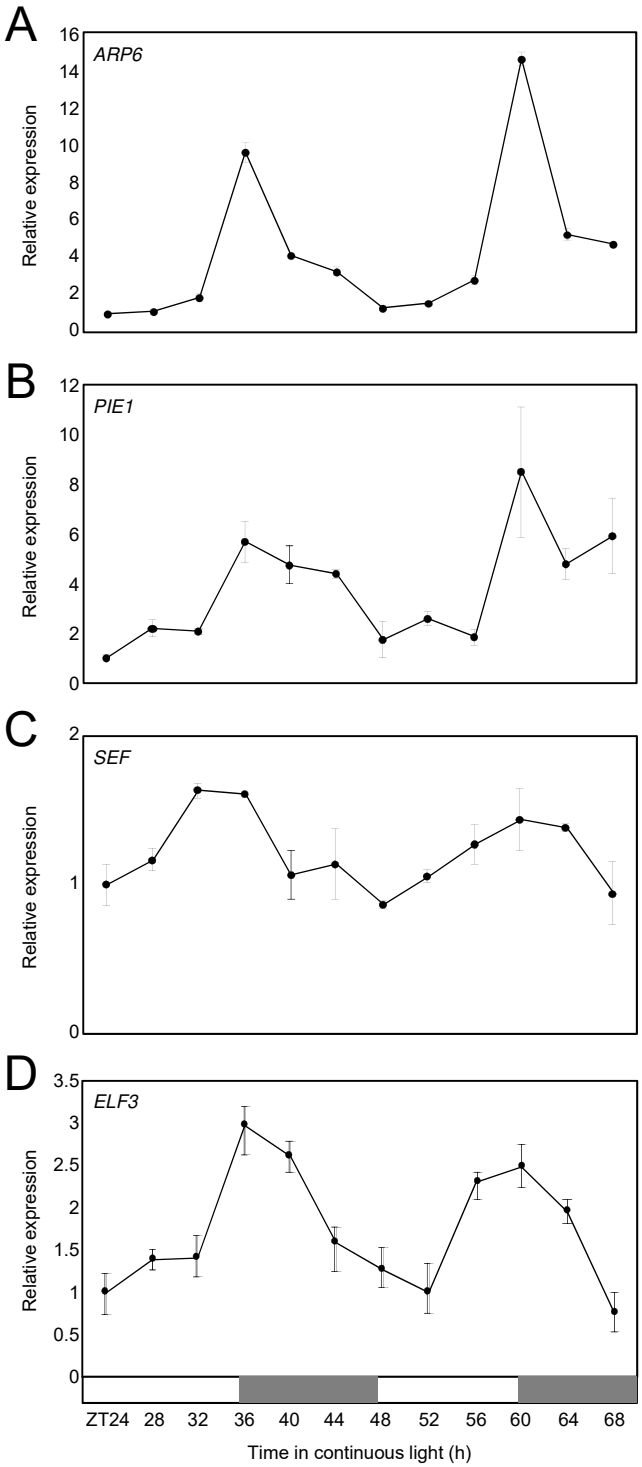

Figure 3

A

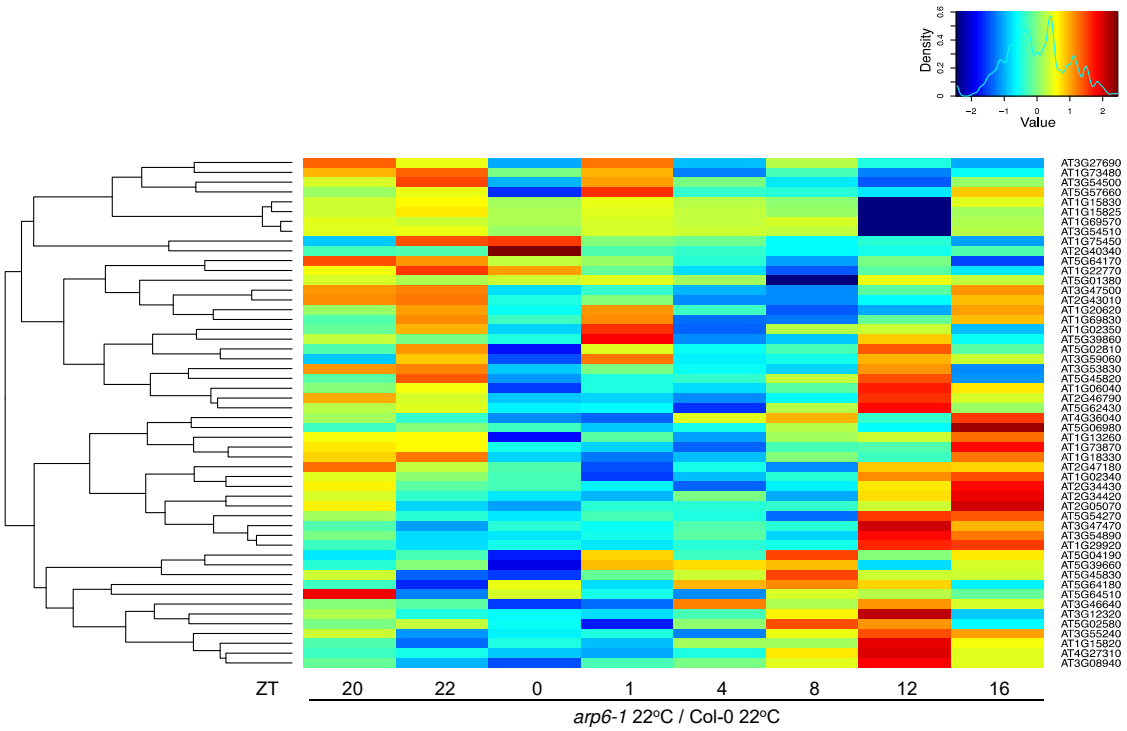

B

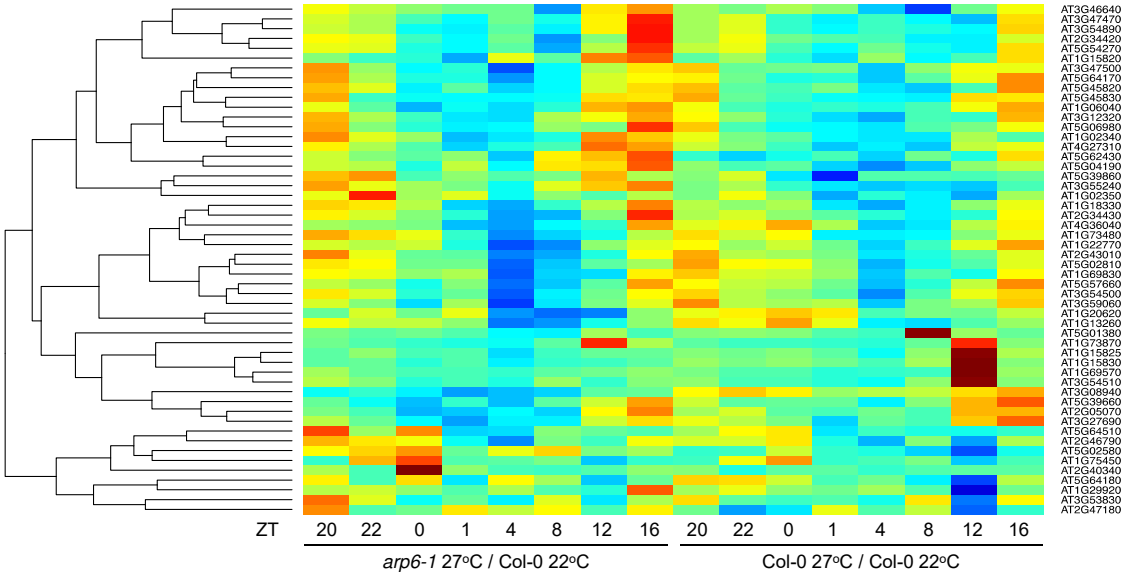

Figure 4

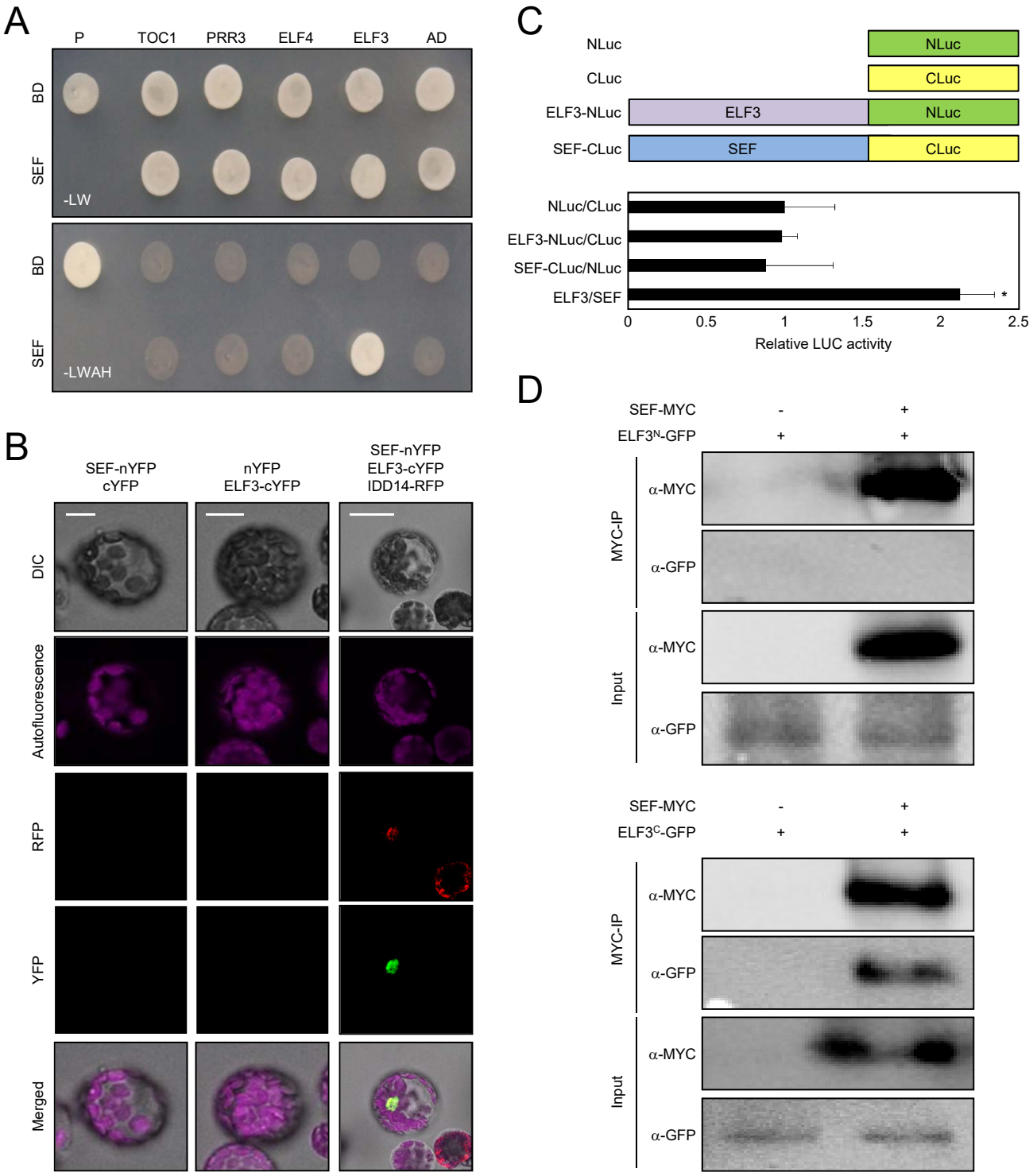

Figure 5

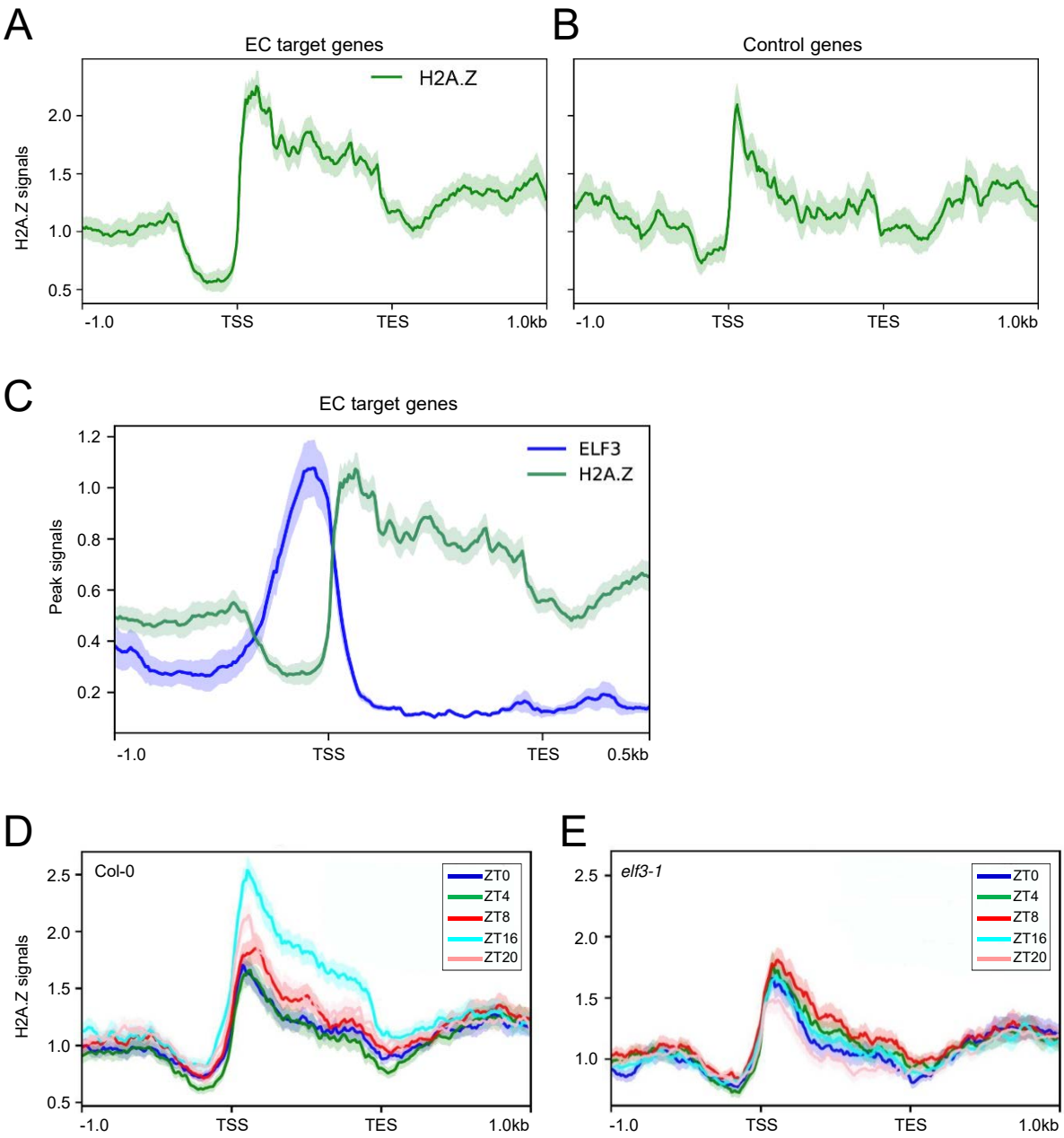

Figure 6

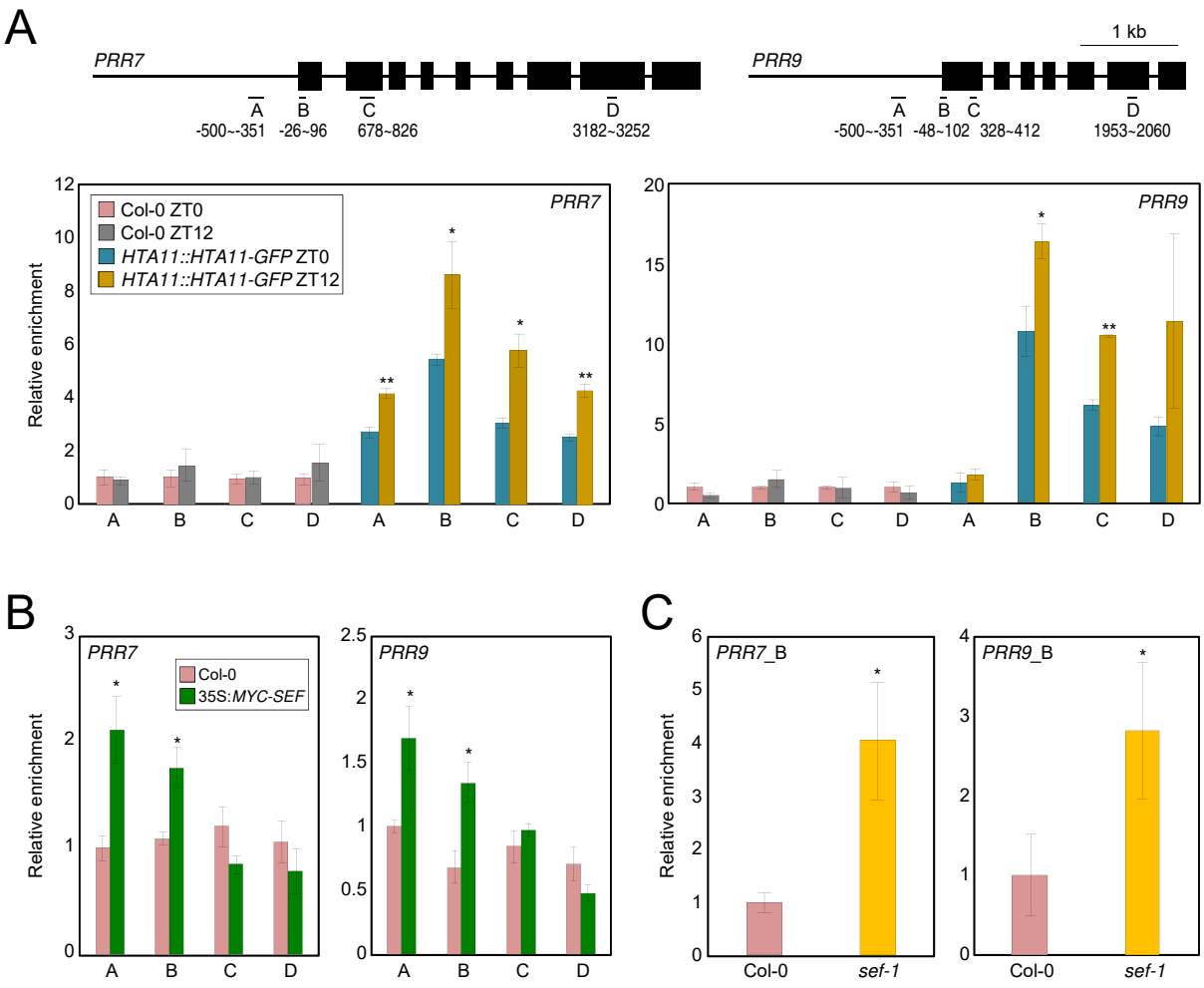

Figure 7

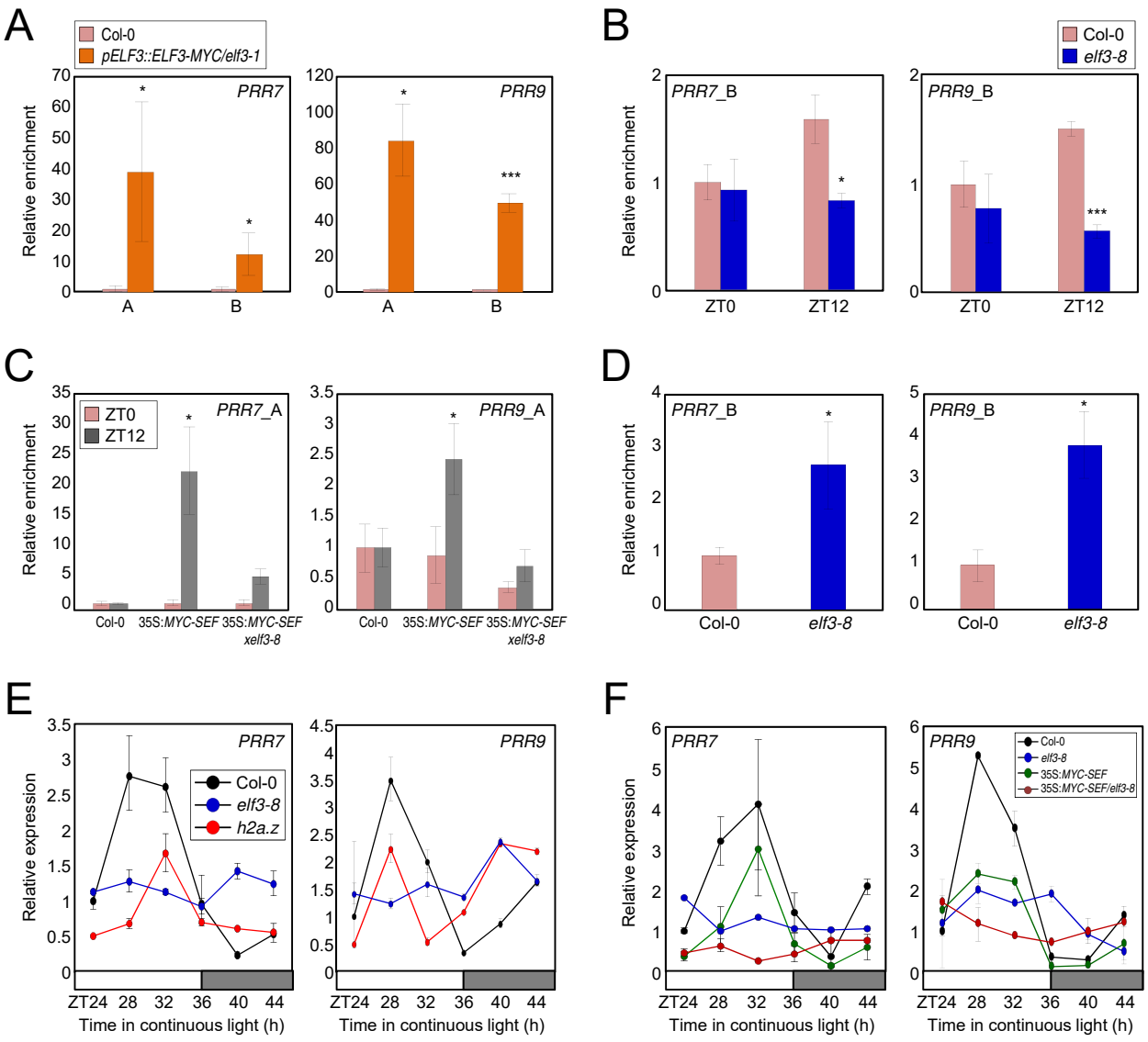

Parsed Citations

Alabadi D, Oyama T, Yanovsky MJ, Harmon FG, Mas P, Kay SA (2001) Reciprocal regulation between TOC1 and LHY/CCA1 within the Arabidopsis circadian clock. Science 293: 880-883

Pubmed: Author and Title
Google Scholar: Author Only Title Only Author and Title

Anders S, Pyl PT, Huber W (2015) HTSeq--a Python framework to work with high-throughput sequencing data. Bioinformatics 31: 166-169

Pubmed: Author and Title
Google Scholar: Author Only Title Only Author and Title

Bolger AM, Lohse M, Usadel B (2014) Trimmomatic: a flexible trimmer for Illumina sequence data. Bioinformatics 30: 2114-2120

Pubmed: Author and Title
Google Scholar: Author Only Title Only Author and Title

Box MS, Huang BE, Domijan M, Jaeger KE, Khattak AK, Yoo SJ, Sedivy EL, Jones DM, Hearn TJ, Webb AA, Grant A, Locke JC, Wigge PA (2015) ELF3 controls thermoresponsive growth in Arabidopsis. Curr Biol 25: 194-199

Pubmed: Author and Title
Google Scholar: Author Only Title Only Author and Title

Carre IA, Kim JY (2002) MYB transcription factors in the Arabidopsis circadian clock. J Exp Bot 53: 1551-1557

Pubmed: Author and Title
Google Scholar: Author Only Title Only Author and Title

Chen K, Xi Y, Pan X, Li Z, Kaestner K, Tyler J, Dent S, He X, Li W (2013) DANPOS: dynamic analysis of nucleosome position and occupancy by sequencing. Genome Res 23: 341-351

Pubmed: Author and Title
Google Scholar: Author Only Title Only Author and Title

Chow BY, Helfer A, Nusinow DA, Kay SA (2012) ELF3 recruitment to the PRR9 promoter requires other Evening Complex members in the Arabidopsis circadian clock. Plant Signal Behav 7: 170-173

Pubmed: Author and Title
Google Scholar: Author Only Title Only Author and Title

Coleman-Derr D, Zilberman D (2012) Deposition of histone variant H2A.Z within gene bodies regulates responsive genes. PLoS Genet 8: e1002988

Pubmed: Author and Title
Google Scholar: Author Only Title Only Author and Title

Cortijo S, Charoensawan V, Brestovitsky A, Buning R, Ravarani C, Rhodes D, van Noort J, Jaeger KE, Wigge PA (2017) Transcriptional Regulation of the Ambient Temperature Response by H2A.Z Nucleosomes and HSF1 Transcription Factors in Arabidopsis. Mol Plant 10: 1258-1273

Pubmed: Author and Title
Google Scholar: Author Only Title Only Author and Title

Deal RB, Kandasamy MK, McKinney EC, Meagher RB (2005) The nuclear actin-related protein ARP6 is a pleiotropic developmental regulator required for the maintenance of FLOWERING LOCUS C expression and repression of flowering in Arabidopsis. Plant Cell 17: 2633-2646

Pubmed: Author and Title
Google Scholar: Author Only Title Only Author and Title

Deal RB, Topp CN, McKinney EC, Meagher RB (2007) Repression of flowering in Arabidopsis requires activation of FLOWERING LOCUS C expression by the histone variant H2A.Z. Plant Cell 19: 74-83

Pubmed: Author and Title
Google Scholar: Author Only Title Only Author and Title

Ezer D, Jung JH, Lan H, Biswas S, Gregoire L, Box MS, Charoensawan V, Cortijo S, Lai X, Stockle D, Zubieta C, Jaeger KE, Wigge PA (2017) The evening complex coordinates environmental and endogenous signals in Arabidopsis. Nat. Plants 3: 17087

Pubmed: Author and Title
Google Scholar: Author Only Title Only Author and Title

Farinas B, Mas P (2011) Functional implication of the MYB transcription factor RVE8/LCL5 in the circadian control of histone acetylation. Plant J 66: 318-329

Pubmed: Author and Title
Google Scholar: Author Only Title Only Author and Title

Farre EM, Harmer SL, Harmon FG, Yanovsky MJ, Kay SA (2005) Overlapping and distinct roles of PRR7 and PRR9 in the Arabidopsis circadian clock. Curr Biol 15: 47-54

Pubmed: Author and Title
Google Scholar: Author Only Title Only Author and Title

Gendron JM, Pruneda-Paz JL, Doherty CJ, Gross AM, Kang SE, Kay SA (2012) Arabidopsis circadian clock protein, TOC1, is a DNA-binding transcription factor. Proc Natl Acad Sci U S A 109: 3167-3172

Pubmed: Author and Title
Google Scholar: Author Only Title Only Author and Title

Greenham K, McClung CR (2015) Integrating circadian dynamics with physiological processes in plants. Nat Rev Genet 16: 598-610
Pubmed: Author and Title
Google Scholar: Author Only Title Only Author and Title

Guillemette B, Bataille AR, Gevry N, Adam M, Blanchette M, Robert F, Gaudreau L (2005) Variant histone H2A.Z is globally localized to the promoters of inactive yeast genes and regulates nucleosome positioning. PLoS Biol 3: e384
Pubmed: Author and Title
Google Scholar: Author Only Title Only Author and Title

Hazen SP, Schultz TF, Pruneda-Paz JL, Borevitz JO, Ecker JR, Kay SA (2005) LUX ARRHYTHMO encodes a Myb domain protein essential for circadian rhythms. Proc Natl Acad Sci U S A 102: 10387-10392
Pubmed: Author and Title
Google Scholar: Author Only Title Only Author and Title

Herrero E, Kolmos E, Bujdoso N, Yuan Y, Wang M, Berns MC, Uhlworm H, Coupland G, Saini R, Jaskolski M, Webb A, Goncalves J, Davis SJ (2012) EARLY FLOWERING4 recruitment of EARLY FLOWERING3 in the nucleus sustains the Arabidopsis circadian clock. Plant Cell 24: 428-443
Pubmed: Author and Title
Google Scholar: Author Only Title Only Author and Title

Hicks KA, Albertson TM, Wagner DR (2001) EARLY FLOWERING3 encodes a novel protein that regulates circadian clock function and flowering in Arabidopsis. Plant Cell 13: 1281-1292
Pubmed: Author and Title
Google Scholar: Author Only Title Only Author and Title

Hicks KA, Millar AJ, Carre IA, Somers DE, Straume M, Meeks-Wagner DR, Kay SA (1996) Conditional circadian dysfunction of the Arabidopsis early-flowering 3 mutant. Science 274: 790-792
Pubmed: Author and Title
Google Scholar: Author Only Title Only Author and Title

Hsu PY, Devisetty UK, Harmer SL (2013) Accurate timekeeping is controlled by a cycling activator in Arabidopsis. Elife 2: e00473
Pubmed: Author and Title
Google Scholar: Author Only Title Only Author and Title

Huang H, Alvarez S, Bindbeutel R, Shen Z, Naldrett MJ, Evans BS, Briggs SP, Hicks LM, Kay SA, Nusinow DA (2016) Identification of Evening Complex Associated Proteins in Arabidopsis by Affinity Purification and Mass Spectrometry. Mol Cell Proteomics 15: 201-217
Pubmed: Author and Title
Google Scholar: Author Only Title Only Author and Title

Huang H, Nusinow DA (2016) Into the Evening: Complex Interactions in the Arabidopsis Circadian Clock. Trends Genet 32: 674-686
Pubmed: Author and Title
Google Scholar: Author Only Title Only Author and Title

Huang W, Perez-Garcia P, Pokhilko A, Millar AJ, Antoshechkin I, Riechmann JL, Mas P (2012) Mapping the core of the Arabidopsis circadian clock defines the network structure of the oscillator. Science 336: 75-79
Pubmed: Author and Title
Google Scholar: Author Only Title Only Author and Title

Jang K, Lee HG, Jung SJ, Paek NC, Seo PJ (2015) The E3 Ubiquitin Ligase COP1 Regulates Thermosensory Flowering by Triggering GI Degradation in Arabidopsis. Sci Rep 5: 12071
Pubmed: Author and Title
Google Scholar: Author Only Title Only Author and Title

Jones MA, Harmer S (2011) JMJD5 Functions in concert with TOC1 in the arabidopsis circadian system. Plant Signal Behav 6: 445-448
Pubmed: Author and Title
Google Scholar: Author Only Title Only Author and Title

Kumar SV, Wigge PA (2010) H2A.Z-containing nucleosomes mediate the thermosensory response in Arabidopsis. Cell 140: 136-147
Pubmed: Author and Title
Google Scholar: Author Only Title Only Author and Title

Langmead B, Salzberg SL (2012) Fast gapped-read alignment with Bowtie 2. Nat Methods 9: 357-359
Pubmed: Author and Title
Google Scholar: Author Only Title Only Author and Title

Lu SX, Knowles SM, Webb CJ, Celaya RB, Cha C, Siu JP, Tobin EM (2011) The Jumonji C domain-containing protein JMJ30 regulates period length in the Arabidopsis circadian clock. Plant Physiol 155: 906-915
Pubmed: Author and Title
Google Scholar: Author Only Title Only Author and Title

Lu SX, Webb CJ, Knowles SM, Kim SH, Wang Z, Tobin EM (2012) CCA1 and ELF3 Interact in the control of hypocotyl length and flowering time in Arabidopsis. Plant Physiol 158: 1079-1088

Pubmed: Author and Title
Google Scholar: Author Only Title Only Author and Title

Malapeira J, Khaitova LC, Mas P (2012) Ordered changes in histone modifications at the core of the Arabidopsis circadian clock. Proc Natl Acad Sci U S A 109: 21540-21545
Pubmed: Author and Title
Google Scholar: Author Only Title Only Author and Title

March-Diaz R, Garcia-Dominguez M, Florencio FJ, Reyes JC (2007) SEF, a new protein required for flowering repression in Arabidopsis, interacts with PIE1 and ARP6. Plant Physiol 143: 893-901
Pubmed: Author and Title
Google Scholar: Author Only Title Only Author and Title

March-Diaz R, Reyes JC (2009) The beauty of being a variant: H2A.Z and the SWR1 complex in plants. Mol Plant 2: 565-577
Pubmed: Author and Title
Google Scholar: Author Only Title Only Author and Title

Menet JS, Pescatore S, Rosbash M (2014) CLOCK:BMAL1 is a pioneer-like transcription factor. Genes Dev 28: 8-13
Pubmed: Author and Title
Google Scholar: Author Only Title Only Author and Title

Nakamichi N, Kiba T, Henriques R, Mizuno T, Chua NH, Sakakibara H (2010) PSEUDO-RESPONSE REGULATORS 9, 7, and 5 are transcriptional repressors in the Arabidopsis circadian clock. Plant Cell 22: 594-605
Pubmed: Author and Title
Google Scholar: Author Only Title Only Author and Title

Nitschke S, Cortleven A, Iven T, Feussner I, Havaux M, Riefler M, Schmulling T (2016) Circadian Stress Regimes Affect the Circadian Clock and Cause Jasmonic Acid-Dependent Cell Death in Cytokinin-Deficient Arabidopsis Plants. Plant Cell 28: 1616-1639
Pubmed: Author and Title
Google Scholar: Author Only Title Only Author and Title

Noh YS, Amasino RM (2003) PIE1, an ISWI family gene, is required for FLC activation and floral repression in Arabidopsis. Plant Cell 15: 1671-1682
Pubmed: Author and Title
Google Scholar: Author Only Title Only Author and Title

Nusinow DA, Helfer A, Hamilton EE, King JJ, Imaizumi T, Schultz TF, Farre EM, Kay SA (2011) The ELF4-ELF3-LUX complex links the circadian clock to diurnal control of hypocotyl growth. Nature 475: 398-402
Pubmed: Author and Title
Google Scholar: Author Only Title Only Author and Title

Perales M, Mas P (2007) A functional link between rhythmic changes in chromatin structure and the Arabidopsis biological clock. Plant Cell 19: 2111-2123
Pubmed: Author and Title
Google Scholar: Author Only Title Only Author and Title

Pokhilko A, Mas P, Millar AJ (2013) Modelling the widespread effects of TOC1 signalling on the plant circadian clock and its outputs. BMC Syst Biol 7: 23
Pubmed: Author and Title
Google Scholar: Author Only Title Only Author and Title

Raisner RM, Hartley PD, Meneghini MD, Bao MZ, Liu CL, Schreiber SL, Rando OJ, Madhani HD (2005) Histone variant H2A.Z marks the 5' ends of both active and inactive genes in euchromatin. Cell 123: 233-248
Pubmed: Author and Title
Google Scholar: Author Only Title Only Author and Title

Raisner RM, Madhani HD (2006) Patterning chromatin: form and function for H2A.Z variant nucleosomes. Curr Opin Genet Dev 16: 119-124
Pubmed: Author and Title
Google Scholar: Author Only Title Only Author and Title

Ramirez F, Dundar F, Diehl S, Gruning BA, Manke T (2014) deepTools: a flexible platform for exploring deep-sequencing data. Nucleic Acids Res 42: W187-191
Pubmed: Author and Title
Google Scholar: Author Only Title Only Author and Title

Rangasamy D, Berven L, Ridgway P, Tremethick DJ (2003) Pericentric heterochromatin becomes enriched with H2A.Z during early mammalian development. EMBO J 22: 1599-1607
Pubmed: Author and Title
Google Scholar: Author Only Title Only Author and Title

Rosa M, Von Harder M, Cigliano RA, Schlogelhofer P, Mittelsten Scheid O (2013) The Arabidopsis SWR1 chromatin-remodeling complex is important for DNA repair, somatic recombination, and meiosis. Plant Cell 25: 1990-2001
Pubmed: Author and Title
Google Scholar: Author Only Title Only Author and Title

Salome PA, McClung CR (2004) The Arabidopsis thaliana clock. J Biol Rhythms 19: 425-435
Pubmed: Author and Title
Google Scholar: Author Only Title Only Author and Title

Salome PA, Weigel D, McClung CR (2010) The role of the Arabidopsis morning loop components CCA1, LHY, PRR7, and PRR9 in temperature compensation. Plant Cell 22: 3650-3661
Pubmed: Author and Title
Google Scholar: Author Only Title Only Author and Title

Seo PJ, Mas P (2014) Multiple layers of posttranslational regulation refine circadian clock activity in Arabidopsis. Plant Cell 26: 79-87
Pubmed: Author and Title
Google Scholar: Author Only Title Only Author and Title

Seo PJ, Mas P (2015) STRESSing the role of the plant circadian clock. Trends Plant Sci 20: 230-237
Pubmed: Author and Title
Google Scholar: Author Only Title Only Author and Title

Shu H, Gruissem W, Hennig L (2013) Measuring Arabidopsis chromatin accessibility using DNase I-polymerase chain reaction and DNase I-chip assays. Plant Physiol 162: 1794-1801
Pubmed: Author and Title
Google Scholar: Author Only Title Only Author and Title

Song HR, Noh YS (2012) Rhythmic oscillation of histone acetylation and methylation at the Arabidopsis central clock loci. Mol Cells 34: 279-287
Pubmed: Author and Title
Google Scholar: Author Only Title Only Author and Title

Staiger D, Green R (2011) RNA-based regulation in the plant circadian clock. Trends Plant Sci 16: 517-523
Pubmed: Author and Title
Google Scholar: Author Only Title Only Author and Title

Swaminathan J, Baxter EM, Corces VG (2005) The role of histone H2Av variant replacement and histone H4 acetylation in the establishment of Drosophila heterochromatin. Genes Dev 19: 65-76
Pubmed: Author and Title
Google Scholar: Author Only Title Only Author and Title

Thakar A, Gupta P, McAllister WT, Zlatanova J (2010) Histone variant H2A.Z inhibits transcription in reconstituted nucleosomes. Biochemistry 49: 4018-4026
Pubmed: Author and Title
Google Scholar: Author Only Title Only Author and Title

To TK, Kim JM (2014) Epigenetic regulation of gene responsiveness in Arabidopsis. Front Plant Sci 4: 548
Pubmed: Author and Title
Google Scholar: Author Only Title Only Author and Title

Trapnell C, Pachter L, Salzberg SL (2009) TopHat: discovering splice junctions with RNA-Seq. Bioinformatics 25: 1105-1111
Pubmed: Author and Title
Google Scholar: Author Only Title Only Author and Title

Voss U, Wilson MH, Kenobi K, Gould PD, Robertson FC, Peer WA, Lucas M, Swarup K, Casimiro I, Holman TJ, Wells DM, Peret B, Goh T, Fukaki H, Hodgman TC, Laplaze L, Halliday KJ, Ljung K, Murphy AS, Hall AJ, Webb AA, Bennett MJ (2015) The circadian clock rephases during lateral root organ initiation in Arabidopsis thaliana. Nat Commun 6: 7641
Pubmed: Author and Title
Google Scholar: Author Only Title Only Author and Title

Wang L, Kim J, Somers DE (2013) Transcriptional corepressor TOPLESS complexes with pseudoresponse regulator proteins and histone deacetylases to regulate circadian transcription. Proc Natl Acad Sci U S A 110: 761-766
Pubmed: Author and Title
Google Scholar: Author Only Title Only Author and Title

Yerushalmi S, Yakir E, Green RM (2011) Circadian clocks and adaptation in Arabidopsis. Mol Ecol 20: 1155-1165
Pubmed: Author and Title
Google Scholar: Author Only Title Only Author and Title